ANNUAL REVIEWS

Annual Review of Fluid Mechanics

Large-Scale Eddy-Mean Flow Interaction in the Earth's Extratropical Atmosphere

Noboru Nakamura

Department of the Geophysical Sciences, University of Chicago, Chicago, USA; email: nnn@uchicago.edu

Annu. Rev. Fluid Mech. 2024. 56:349–77

First published as a Review in Advance on October 3, 2023

The *Annual Review of Fluid Mechanics* is online at fluid.annualreviews.org

https://doi.org/10.1146/annurev-fluid-121021-035602

Keywords

Rossby waves, jet stream, angular momentum budget, potential vorticity, Kelvin's circulation, finite-amplitude wave activity, local wave activity

Abstract

Large-scale circulation of the atmosphere in the Earth's extratropics is dominated by eddies, eastward (westerly) zonal winds, and their interaction. Eddies not only bring about weather variabilities but also help maintain the average state of climate. In recent years, our understanding of how large-scale eddies and mean flows interact in the extratropical atmosphere has advanced significantly due to new dynamical constraints on finite-amplitude eddies and the related eddy-free reference state. This article reviews the theoretical foundations for finite-amplitude Rossby wave activity and related concepts. Theory is then applied to atmospheric data to elucidate how angular momentum is redistributed by the generation, transmission, and dissipation of Rossby waves and to reveal how an anomalously large wave event such as atmospheric blocking may arise from regional eddy-mean flow interaction.

1. INTRODUCTION

Troposphere: weather layer of the atmosphere that occupies from the ground up to about 11 km in altitude on average

Jet stream: fast eastward winds that dominate the mid- to upper troposphere (5–10 km above sea level)

Weather and climate variabilities in the Earth's midlatitudes (30–60°) affect the lives of billions. The spatio-temporal structure of atmospheric circulation that drives these variabilities is dominated by large-scale eddies (weather systems) and an eastward mean flow that steers them. In the upper troposphere, they manifest themselves as a meandering jet stream (**Figure 1*a***). How eddies and the mean flow interact with each other is central to our understanding of weather and climate in the extratropics, and it has been a main theme of atmospheric dynamics for decades (Hartmann 2015, Vallis 2017, Wallace et al. 2023).

Linear wave theory explains the origin and propagation of the waveforms in large-scale eddies known as the Rossby waves (Rossby 1939, Haurwitz 1940, Longuet-Higgins 1965, Platzman 1968). The Rossby waves arise from hydrodynamic instabilities of the zonal-mean state such as baroclinic instability (Charney 1947, Eady 1949, Phillips 1951) or from external forcing such as form stress of topography (Eliassen & Palm 1961, Hoskins & Karoly 1981, Held 1983). The mean flow then regulates the dispersion of the generated waves. The waves in turn modify the mean flow by redistributing angular momentum through their radiation stress and the wave-induced circulation (Eliassen 1951; Kuo 1956; Charney & Drazin 1961; Eliassen & Palm 1961; Dickinson 1968,

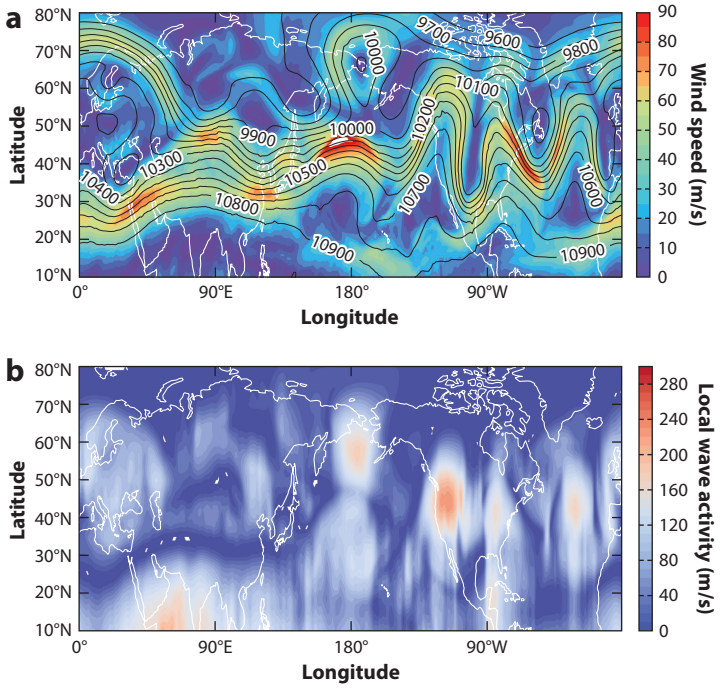

Figure 1

(*a*) Jet stream in the upper troposphere of the Northern Hemisphere on March 23, 2022 (00 UTC). The map shows geopotential height Z (altitude; *contours* in meters) and horizontal wind speed $(u^2 + v^2)^{1/2}$ (*color* in ms^{-1}) for the 250 hPa pressure surface. At this altitude, geopotential height is approximately a streamfunction according to the geostrophic balance, so the winds blow parallel to Z eastward. Large-scale eddies create chaotic meandering of the eastward jet stream, a manifestation of Rossby waves. (*b*) Same as panel *a* but for local wave activity (Huang & Nakamura 2016), which equals negative angular pseudomomentum density carried by eddies. Data from European Centre for Medium-Range Weather Forecasts Reanalysis v5 (Hersbach et al. 2020).

1970; Rhines 1975; Andrews & McIntyre 1976; Boyd 1976; Salmon 1980). Changes in angular momentum distribution also alter heat distribution because in large-scale circulations of rapidly rotating atmospheres, momentum and temperature are related through thermal wind balance. Theory of eddy-mean flow interaction resolved some key questions—for example, why surface westerlies in the extratropics can be maintained against friction (Jeffreys 1926, Held & Hoskins 1985) and what causes stratospheric sudden warming (Matsuno 1971).

While much progress was made in the latter half of the previous century, certain gaps still remained between the theory of eddy-mean flow interaction and its application to meteorological data. For one, although the theory for the zonal-mean zonal circulation and its response to eddy forcing was fully developed, the corresponding theory for eddy and its role in redistributing angular momentum and heat was mostly linear and thus limited to small-amplitude eddy. Finite-amplitude theory was developed but not in a form readily applicable to atmospheric data. As a result, unlike the Lorenz energy cycle (Lorenz 1955), the angular momentum cycle between eddy and the mean flow was not closed, leaving some key questions unanswered: e.g., how much is the observed zonal-mean state already modified by the eddy effects and to what extent are nonconservative processes (e.g., wave dissipation and/or diabatic heating) responsible for the observed angular momentum distribution?

In recent years some advances have been made, and one can now evaluate and map the amount of angular pseudomomentum carried by finite-amplitude Rossby waves (**Figure 1*b***; for details, see Section 3) and its regional budget (Section 4). Not only does this help close the angular momentum cycle, but also it identifies the conditions conducive to large-amplitude wave events driven by eddy-mean flow interaction. In this article I review the theoretical framework behind this new development and highlight its applications to meteorological data. To set the stage, I start with a brief review of fundamentals. For a more complete introduction to the subject, see, for example, chapter 10 of Vallis (2017).

Rossby waves: horizontal undulation of the flow in a rotating fluid due to meridional gradient of vorticity

Baroclinic instability: instability of a rotating stratified fluid in the presence of meridional density gradient

Thermal wind balance: balance between vertical wind shear and horizontal temperature gradient that arises from hydrostatic and geostrophic balance of forces

Stratospheric sudden warming: major disruption of the stratospheric polar vortex involving reversal of the jet and rapid warming

Lorenz energy cycle: 4-component cycle that defines the partition and transfer of energy between the zonal-mean state and eddy field, as well as between kinetic and available potential energy

Angular pseudomomentum: average angular momentum carried by the wave field, or the wave's ability to modify the angular momentum of the mean flow

2. FUNDAMENTALS

Due partly to the strong height and latitude dependence of the atmospheric state and partly to the ease of application to gridded data, it is common to adopt longitudinal (zonal) averaging to define the mean state and the local departure from the zonal mean to define eddy. In this article I denote the zonal mean by an overbar and eddy by a prime:

$$W(x,y,z,t) = \overline{W}(y,z,t) + W'(x,y,z,t), \qquad 1.$$

where W is any field variable in the Cartesian coordinate (x, y, z), where x is longitude, y is latitude, $z \equiv -H\ln(p/p_0)$ is pressure pseudoheight (H is constant scale height and $p_0 = 1{,}000$ hPa), and t is time. (I introduce a spherical coordinate suitable for data analysis in Section 3.) W is assumed to be cyclic in x. Equation 1 is a special form of Reynolds decomposition. It is not the only way to define eddy and mean, and later I introduce a new definition of eddy incorporating a (quasi-)Lagrangian coordinate. Such freedom in the choice of coordinate proves essential for making progress in theory.

2.1. Quasigeostrophic Approximation

The first step is to simplify the governing equations for the analysis of extratropical circulation. In the Earth's extratropics, the evolution of the large-scale circulation of the atmosphere is slower than the rotation of the planet with respect to the local vertical axis. By assuming that the atmospheric state is a small perturbation to a (constant) solid body rotation and to a horizontally uniform stable stratification, one can apply perturbation theory to the equations of motion and first

thermodynamics to derive quasigeostrophic dynamics. Quasigeostrophy is an approximate state of the atmosphere that evolves slowly maintaining hydrostatic and geostrophic balance, wherein pressure (streamfunction ψ) becomes the sole variable in the fluid interior. Horizontal winds and temperature simply become gradients of ψ. Acoustic and inertia-gravity waves are filtered out. The quasigeostrophic dynamics is governed by the material conservation and invertibility of potential vorticity (PV) q:

Pressure pseudoheight: a scaled pressure coordinate that approximates altitude under hydrostatic assumption while eliminating density as a dynamic variable

Potential vorticity (PV): a materially conserved dynamic tracer in adiabatic, frictionless flow (a differential form of Kelvin's circulation); q in Equation 4 is a quasigeostrophic approximation to PV

Wentzel–Kramers–Brillouin (WKB) approximation: mathematical approximation to describe a wave train traveling in a slowly varying medium, with modulations in the wave structure

$$\frac{D_g}{Dt} q = \dot{q}, \tag{2.}$$

$$\frac{D_g}{Dt} = \frac{\partial}{\partial t} - \frac{\partial \psi}{\partial y}\frac{\partial}{\partial x} + \frac{\partial \psi}{\partial x}\frac{\partial}{\partial y}, \tag{3.}$$

$$q(x,y,z,t) = \beta y + \nabla_{\mathrm{H}}^2 \psi + \frac{f_0^2}{\rho_0(z)}\frac{\partial}{\partial z}\left(\frac{\rho_0(z)}{N_0^2(z)}\frac{\partial \psi}{\partial z}\right), \tag{4.}$$

where $\dot{q}$ is nonconservative sources and sinks of q, $f = f_0 + \beta y$ is the latitude-dependent Coriolis parameter (= twice the rate of planetary rotation about the local vertical axis), $\rho_0(z) \propto e^{-z/H}$ is background density, $N_0^2(z)$ is the squared buoyancy frequency, and ∇_{H}^2 is horizontal Laplacian (see, e.g., Charney 1948, section 3.2.3 of Andrews et al. 1987). To invert ψ from q with Equation 4, one needs boundary conditions. In particular, at the lower boundary a separate prediction of $\partial\psi/\partial z$ is needed with the help of the thermodynamic equation.

2.2. Rossby Waves in a Slowly Varying Flow

The rudimentary behavior of the Rossby waves in the midlatitude atmosphere is described by the quasigeostrophic PV equation linearized about a steady zonal-mean state. By substituting $q = \overline{q}(y,z) + q'(x,y,z,t)$ and $\psi = \overline{\psi}(y,z) + \psi'(x,y,z,t)$ in Equation 2, one obtains an eddy PV equation,

$$\frac{\partial q'}{\partial t} + \overline{u}\frac{\partial q'}{\partial x} + \frac{\partial \psi'}{\partial x}\frac{\partial \overline{q}}{\partial y} = O(\alpha^2) + \dot{q}', \tag{5.}$$

$$q' = \nabla_{\mathrm{H}}^2 \psi' + \frac{f_0^2}{\rho_0}\frac{\partial}{\partial z}\left(\frac{\rho_0}{N_0^2}\frac{\partial \psi'}{\partial z}\right), \qquad \overline{u} = -\frac{\partial \overline{\psi}}{\partial y}, \tag{6.}$$

$$\frac{\partial \overline{q}}{\partial y} = \beta - \frac{\partial^2 \overline{u}}{\partial y^2} - \frac{f_0^2}{\rho_0}\frac{\partial}{\partial z}\left(\frac{\rho_0}{N_0^2}\frac{\partial \overline{u}}{\partial z}\right), \tag{7.}$$

where α denotes the amplitude of eddy. Now linearize the equation by discarding the right-hand side (RHS) terms of Equation 5. If one assumes that $\overline{u}$, $\partial\overline{q}/\partial y$, and the wave amplitude vary in the meridional plane only slowly compared to the scale of the wavelength [the Wentzel–Kramers–Brillouin (WKB) approximation] and that N_0^2 also varies smoothly and slowly over the scale height H, Equation 5 accepts a monochromatic waveform modulated over the slow scale $(Y, Z) \equiv \epsilon(y, z)$ $(\epsilon \ll 1)$:

$$\psi' = \Psi(Y,Z) e^{i\Theta(Y,Z)/\epsilon} e^{z/2H} e^{i(kx-\omega t)}, \tag{8.}$$

where

$$\frac{\partial \Theta}{\partial Y} = l(Y,Z), \quad \frac{\partial \Theta}{\partial Z} = m(Y,Z) \tag{9.}$$

define the modulated wavenumbers. The zonal wavenumber k and frequency ω are constant, consistent with the zonally uniform, steady background. Substituting in Equation 5 and collecting the

real part to the leading order, one obtains a local WKB dispersion relation,

$$\omega = \overline{u}k - \frac{k\partial\overline{q}/\partial y}{k^2 + l^2 + \frac{f_0^2}{N_0^2}\left(m^2 + \frac{1}{4H^2}\right)}, \qquad 10.$$

while from the imaginary part a constraint on the wave amplitude Ψ along the ray emerges:

$$\frac{\partial}{\partial Y}\left(l\Psi^2\right) + \frac{\partial}{\partial Z}\left(\frac{f_0^2}{N_0^2}m\Psi^2\right) = 0. \qquad 11.$$

Since $\partial\overline{q}/\partial y$ is usually dominated by the gradient of the Coriolis parameter $\beta > 0$, Equation 10 shows that the zonal phase speed of the Rossby wave $c = \omega/k$ is slower than $\overline{u}$ (i.e., westward with respect to the zonal-mean zonal wind). This is because the flow induced by the eddy PV gives rise to meridional advection of the background PV (the third term of Equation 5), which produces a tendency of q' opposite of eastward zonal advection (second term), known as the β-effect.

Hamiltonian formulation of wave dynamics: formulation in which the dispersion relation and amplitude equation of the waves are derived from the principle of stationary action applied to the average Lagrangian density

2.3. Generalized Eliassen-Palm Theorem

A key role of Rossby waves is to transmit zonal pseudomomentum (in the spherical coordinate this is generalized to angular pseudomomentum, with a multiplication factor $a\cos\phi$, where a is the radius of the planet and ϕ is latitude relative to the Equator) from the wave source region to a remote sink, where the momentum is deposited to the mean flow. Characterization of atmospheric waves as a transmitter of pseudomomentum originated from the work of Eliassen & Palm (1961) and was later generalized by Andrews & McIntyre (1976, 1978b).

According to the Hamiltonian formulation of wave dynamics, pseudomomentum density carried by a small-amplitude wave traveling through a zonally uniform medium is given by $E/(c-\overline{u})$, where E is energy density of the wave (Bretherton & Garrett 1968). In the present case, $E = \frac{1}{2}[k^2 + l^2 + (f_0^2/N_0^2)(m^2 + \frac{1}{4H^2})]\overline{\psi'^2}$ and by using Equation 8 to rewrite q' in Equation 6 and by incorporating Equation 10, one can show

$$\frac{E}{c-\overline{u}} = -\frac{1}{2}\frac{\overline{q'^2}}{\partial\overline{q}/\partial y} \equiv -A_L. \qquad 12.$$

Since $\partial\overline{q}/\partial y$ is dominated by $\beta > 0$, it follows that $E/(c-\overline{u}) < 0$, viz the Rossby wave carries negative (westward) pseudomomentum. I revisit this point in Section 3.2. The opposite of pseudomomentum density ($A_L > 0$) is called (linear) wave activity. The transmission of wave activity (pseudomomentum) by the Rossby wave is governed by

$$\frac{\partial}{\partial t}A_L = -\overline{v'q'} + O(\alpha^3) + \mathcal{D}, \qquad v' = \frac{\partial\psi'}{\partial x}, \qquad 13.$$

where the first term on the RHS is the meridional flux of eddy PV and $\mathcal{D}$ denotes nonconservative sources and sinks. This equation may be derived by multiplying Equation 5 by q', taking the zonal average, and dividing by $\partial\overline{q}/\partial y$ (which is assumed to be time independent so it goes inside the time derivative). Noting the identity (known as the Taylor–Bretherton identity; it applies to geostrophic eddies of all amplitudes)

$$\overline{v'q'} = \frac{1}{\rho_0}\nabla\cdot\mathbf{F}, \qquad 14.$$

$$\mathbf{F} = \rho_0\left(0, \overline{\frac{\partial\psi'}{\partial x}\frac{\partial\psi'}{\partial y}}, \frac{f_0^2}{N_0^2}\overline{\frac{\partial\psi'}{\partial x}\frac{\partial\psi'}{\partial z}}\right) = \rho_0\left(0, -\overline{u'v'}, \frac{f_0\overline{v'\theta'}}{\mathrm{d}\theta_0/\mathrm{d}z}\right), \qquad 15.$$

where $u' = -\partial\psi'/\partial y$ is eddy zonal wind and θ' and $\theta_0(z)$ are eddy and background potential temperature, Equation 13 becomes

$$\frac{\partial}{\partial t}A_L = -\frac{1}{\rho_0}\nabla\cdot\mathbf{F} + O(\alpha^3) + \mathcal{D}. \qquad 16.$$

The flux $\mathbf{F}$ is called the generalized Eliassen-Palm flux density (E-P flux), and it quantifies the radiation stress of the Rossby wave (Andrews & McIntyre 1976, Edmon et al. 1980). Note that the components of $\mathbf{F}$ have the dimension of momentum flux, but the vertical component is proportional to the meridional eddy heat flux $\overline{v'\theta'}$. With geostrophic balance $v' \propto \partial p'/\partial x$ (p is pressure) and the effective vertical displacement of isentropic surface $\xi' \approx -\theta'/(\mathrm{d}\theta_0/\mathrm{d}z)$, $\overline{v'\theta'}$ is proportional to $\overline{p'\partial\xi'/\partial x}$, i.e., form stress (pressure torque) between adjacent (wavy) isentropic layers. This mode of momentum transfer dominates the vertical momentum flux $-\overline{u'w'}$ in the quasigeostrophic limit. Furthermore, for a small-amplitude wave, by substituting Equation 8 in Equation 15 and by using Equation 10, it is straightforward to show that

$$\mathbf{F} = \rho_0\mathbf{c}_\mathbf{g}A_L, \qquad \mathbf{c}_\mathbf{g} = \left(0, \frac{\partial\omega}{\partial l}, \frac{\partial\omega}{\partial m}\right), \qquad 17.$$

so the E-P flux is the flux of wave activity density (the opposite of pseudomomentum density), which is transported at the group velocity of the Rossby wave in the meridional plane, $\mathbf{c}_\mathbf{g}$. [Although this result is based on the dispersion relation of a monochromatic wave (Equation 10), both linear wave activity A_L and the E-P flux $\mathbf{F}$ permit superposition of multiple wave components. Equations 16 and 17 apply to the superposition of waves if one interprets $\mathbf{c}_\mathbf{g}$ as the average group velocity weighted by wave activity density of the component waves.] Equation 16 is known as the generalized Eliassen–Palm theorem (E-P theorem) (Andrews & McIntyre 1978b, Andrews et al. 1987). It depicts the conservation of wave activity density $\rho_0 A_L$ up to $\mathcal{O}(\alpha^2)$. For a conservative ($\mathcal{D} = 0$) small-amplitude wave, wave activity changes only where $\nabla\cdot\mathbf{F} \neq 0$. However, the WKB wave train traveling in a steady flow does not satisfy this condition because Equation 11 is equivalent to $\nabla\cdot\mathbf{F} = 0$. The inhomogeneity in the mean state modulates the amplitude and wavenumbers of the wave spatially, but the E-P flux remains nondivergent and wave activity remains steady. The only exception is when the wave encounters a critical line $\overline{u} = c$, across which the E-P flux changes discontinuously (e.g., Dickinson 1968, 1970). Thus, the wave transience requires a critical line (at least according to the linear WKB theory; this does not necessarily apply to finite-amplitude eddies).

2.4. Transformed Eulerian Mean Formalism

When the convergence of the E-P flux leads to a change in wave activity, pseudomomentum of the Rossby wave is deposited to the zonal-mean circulation. To the extent that such deposition is frequent and efficient, one expects the zonal-mean circulation of the atmosphere to be substantially altered/driven by the waves. Jeffreys (1926) was among the first to recognize the importance of eddy transport of angular momentum for the maintenance of the general circulation of the atmosphere against surface friction. Yet angular momentum is also transported by the mean meridional (overturning) circulation $(\overline{v}, \overline{w})$, and the relative role of eddies and the overturning circulation in the angular momentum transport became the subject of a colorful debate later (Palmén 1949, Rossby & Starr 1949, Starr 1949).

In the quasigeostrophic limit, zonal-mean zonal wind $\overline{u}$ and potential temperature $\overline{\theta}$ obey

$$\frac{\partial}{\partial t}\overline{u} = f_0\overline{v}_a - \frac{\partial}{\partial y}\overline{u'v'} + \overline{X}, \tag{18.}$$

$$\frac{\partial}{\partial t}\overline{\theta} = -\overline{w}_a\frac{\mathrm{d}\theta_0}{\mathrm{d}z} - \frac{\partial}{\partial y}\overline{v'\theta'} + \overline{\dot{\theta}}, \tag{19.}$$

where $(\overline{v}_a, \overline{w}_a)$ is ageostrophic mean meridional circulation satisfying mass continuity (the form of mass continuity follows from the definition of pressure pseudoheight) $\partial\overline{v}_a/\partial y + \rho_0^{-1}\partial(\rho_0\overline{w}_a)/\partial z = 0$, $\overline{X}$ is the zonal-mean frictional force, and $\overline{\dot{\theta}}$ denotes zonal-mean nonadiabatic heating. Unlike the generalized E-P theorem, Equations 18–22 are exact—that is, eddies need not be of small amplitude. Although Equations 18 and 19 demonstrate that the zonal-mean state of the atmosphere is affected by both the mean meridional circulation and eddy fluxes, the role of the radiation stress of the Rossby wave becomes more transparent if we rewrite the equations in the following form:

$$\frac{\partial}{\partial t}\overline{u} = f_0\overline{v}^* + \frac{1}{\rho_0}\nabla\cdot\mathbf{F} + \overline{X}, \tag{20.}$$

$$\frac{\partial}{\partial t}\overline{\theta} = -\overline{w}^*\frac{\mathrm{d}\theta_0}{\mathrm{d}z} + \overline{\dot{\theta}}, \tag{21.}$$

$$\overline{v}^* = \overline{v}_a - \frac{1}{\rho_0}\frac{\partial}{\partial z}\left(\frac{\rho_0\overline{v'\theta'}}{\mathrm{d}\theta_0/\mathrm{d}z}\right), \quad \overline{w}^* = \overline{w}_a + \frac{\partial}{\partial y}\left(\frac{\overline{v'\theta'}}{\mathrm{d}\theta_0/\mathrm{d}z}\right). \tag{22.}$$

Here $(\overline{v}^*, \overline{w}^*)$ is called the residual circulation. As Equation 21 shows, $\overline{w}^*$ is the effective vertical velocity that advects the zonal-mean isentropes and the difference between $\overline{w}^*$ and $\overline{w}_a$ is akin to the Stokes drift velocity. As we see later in Equation 58, $\overline{v}^*$ is the effective meridional velocity that advects Kelvin's circulation. In this sense, the residual circulation is analogous to the Lagrangian-mean circulation, and it can be significantly different from the Eulerian-mean circulation (Andrews & McIntyre 1976, 1978a). The residual circulation in the troposphere constitutes one overturning cell per hemisphere, rising in the tropics and descending in high latitudes, whereas the Eulerian-mean meridional circulation forms three cells. Note $(\overline{v}^*, \overline{w}^*)$ still satisfies mass continuity $\partial\overline{v}^*/\partial y + \rho_0^{-1}\partial(\rho_0\overline{w}^*)/\partial z = 0$. Equations 20–22 are called the transformed Eulerian mean (TEM) equations (Andrews & McIntyre 1976, Andrews et al. 1987). In the TEM set, $\overline{u}$ and $\overline{\theta}$ are governed by the divergence of the E-P flux (eddy forcing), the residual circulation, and frictional and diabatic forcing. As $\overline{u}$ and $\overline{\theta}$ evolve, they maintain thermal wind balance, whereas the eddy and other forms of forcing tend to disrupt it. The residual circulation plays the role of restoring the thermal wind balance of the zonal-mean state.

In the time average, Equations 16 and 20 become

$$0 = -\frac{1}{\rho_0}\nabla\cdot\mathbf{F} + \mathcal{O}(\alpha^3) + \mathcal{D}, \tag{23.}$$

$$0 = f_0\overline{v}^* + \frac{1}{\rho_0}\nabla\cdot\mathbf{F} + \overline{X}. \tag{24.}$$

Equation 23 states that, apart from the $\mathcal{O}(\alpha^3)$ term, the time-mean E-P flux divergence (convergence) is balanced by the positive (negative) $\mathcal{D}$, meaning that the E-P flux transports wave activity from the wave source region to the wave sink, or transports (positive) pseudomomentum from the wave sink to the wave source. Equation 24 then shows that the E-P flux divergence is balanced by the Coriolis torque of the residual circulation and the frictional force. Friction is generally weak

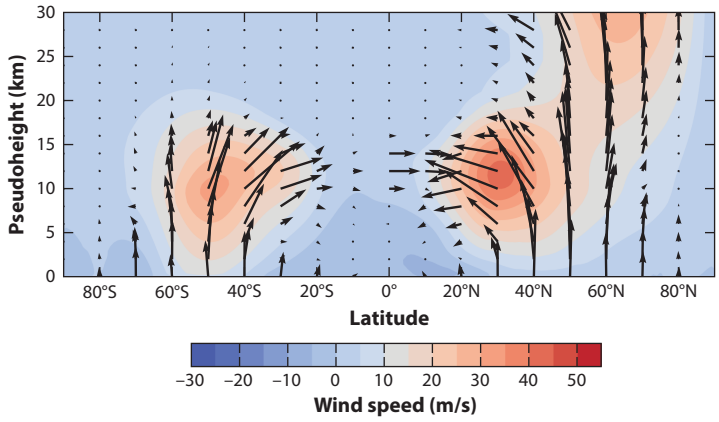

Figure 2

Climatology of the Eliassen-Palm (E-P) flux $\rho_0^{-1}\mathbf{F} = \cos\phi(0, -\overline{u'v'}, f\overline{v'\theta'}/(\mathrm{d}\theta_0/\mathrm{dz}))$ (*arrows*) and the zonal-mean zonal wind $\overline{u}$ (*color*) for December–February as functions of latitude and altitude (pseudoheight). Here ϕ is latitude and $f = 2\Omega\sin\phi$ is the Coriolis parameter ($\Omega = 7.29 \times 10^{-5}$ s^{-1} is the rotation rate of the Earth), $\rho_0(z)$ and $\theta_0(z)$ are the background density and potential temperature, and (u', v', and θ') are the eddy components of zonal and meridional winds and potential temperature. The horizontal to vertical scale for the E-P flux vector is adjusted for an easy visual reference. The upper tropospheric maxima in the zonal-mean zonal wind at ∼30°N and 50°S denote the axes of the jet stream. Data from European Centre for Medium-Range Weather Forecasts Reanalysis v5 (Hersbach et al. 2020).

above the boundary layer, so in the balanced state the wave sink (convergence of the E-P flux) is coincident with a poleward residual circulation.

2.5. Observed Eliassen-Palm Flux Cross Section

Since its introduction by Edmon et al. (1980), the E-P flux cross section remains a popular diagnostic for the flow of wave activity/pseudomomentum in the meridional plane, in no small part because it is easy to compute from gridded meteorological data. **Figure 2** shows the vertical cross section of the average E-P flux vectors in the troposphere and the lower stratosphere for the months of December through February, together with the zonal-mean zonal wind (color). Here I define the E-P flux in the spherical coordinate, where wave activity is the opposite of angular pseudomomentum. The E-P flux is greatest in the midlatitudes, and it points predominantly upward. In both hemispheres, the flux enters the atmosphere from the lower boundary in the midlatitudes. The main source of wave activity at the lower boundary is baroclinic instability, which siphons wave activity from the surface reservoir associated with temperature gradient. Other sources at the surface include form stress of topography and heat exchanges with the ground.

Stratosphere: layer of the atmosphere above the troposphere that extends to about 50 km in altitude; the ozone layer is in the stratosphere

Much of the tropospheric E-P flux is deflected equatorward in the upper troposphere and converges into the subtropics. A smaller fraction of the E-P flux is also deflected to higher latitudes. The convergence of the E-P flux in the flanks of the jet stream suggests that wave activity is dissipated there (Equation 23) due to mixing (wave breaking) associated with critical lines. The pattern of the tropospheric E-P flux largely reflects life cycles of baroclinic waves [baroclinic growth followed by a meridional transmission of synoptic Rossby waves (Held & Hoskins 1985)].

Angular pseudomomentum is transported in the opposite direction of wave activity: It is drawn from the subtropical upper troposphere and transported to the extratropical lower troposphere. The positive (eastward) angular pseudomomentum deposited to the boundary layer is partially balanced by the negative angular momentum advection by the equatorward residual circulation near the surface (Held & Schneider 1999), but it is also balanced by the frictional loss of angular momentum of the zonal-mean flow (Equation 24). From the density-weighted vertical integral of Equation 24, the frictional loss of angular momentum through surface westerlies is balanced by the convergence of the vertically integrated eddy angular momentum flux associated with the meridional radiation of the Rossby waves from the midlatitudes. This resolves the rather counterintuitive observation that the action of eddies is antifrictional, which had puzzled atmospheric scientists for some time (e.g., Starr 1968). It attests to the importance of radiation stress and eventual dissipation of Rossby waves in the maintenance of general circulation.

In the winter Northern Hemisphere, part of the E-P flux enters the stratosphere, where the zonal-mean zonal winds are westerly (color in **Figure 2**). This represents vertical propagation of planetary-scale Rossby waves forced by large land masses in the Northern Hemisphere (Charney & Drazin 1961), distinct from baroclinic instability.

Overall, when averaged globally, wave activity is injected at the lower boundary and dissipated in various parts of the atmosphere through mixing and radiative damping.

2.6. Nonacceleration Theorem

On short timescales, pseudomomentum deposited by the Rossby wave directly alters the zonal-mean zonal wind through the second term on the RHS of Equation 20. However, even if one ignores friction $\overline{X}$, eddy forcing is partly balanced by the Coriolis torque of the residual circulation $f_0\overline{v}^*$. Thus, it is not obvious how much zonal-mean zonal wind will accelerate in response to eddy forcing. A more direct relationship between the zonal acceleration and eddy forcing emerges after one eliminates the residual circulation from Equations 20 and 21 using mass continuity:

$$\left[\frac{\partial^2}{\partial y^2}+\frac{1}{\rho_0}\frac{\partial}{\partial z}\left(\rho_0\varepsilon_0\frac{\partial}{\partial z}\right)\right]\frac{\partial\overline{u}}{\partial t}=\frac{\partial^2}{\partial y^2}\left(\frac{1}{\rho_0}\nabla\cdot\mathbf{F}+\overline{X}\right)-\frac{f_0}{\rho_0}\frac{\partial}{\partial z}\left(\frac{\rho_0}{\mathrm{d}\theta_0/\mathrm{d}z}\frac{\partial\overline{\dot{\theta}}}{\partial y}\right), \qquad 25.$$

where $\varepsilon_0(z)=f_0^2/N_0^2(z)$. In particular, $\partial\overline{u}/\partial t=0$ if $\overline{X}=\overline{\dot{\theta}}=\nabla\cdot\mathbf{F}=0$ and if the boundary conditions are also time independent. (Equation 25 is essentially the equation for the meridional gradient of zonal-mean PV.) Meanwhile, from Equation 16, $\nabla\cdot\mathbf{F}=0$ if $\partial A_L/\partial t=\mathcal{D}=0$ for small-amplitude waves. Therefore, under conservative dynamics ($\overline{X}=\overline{\dot{\theta}}=\mathcal{D}=0$), if the amplitude of wave is small and steady, the zonal-mean zonal wind will not change. This result is known as the nonacceleration theorem (Charney & Drazin 1961, Andrews & McIntyre 1978b). Since the E-P flux divergence appears in both Equations 16 and 25 with opposite signs, these equations establish a generalized action-reaction relation for the zonal-mean zonal wind and the Rossby wave. This result is extended to finite-amplitude eddy in Sections 3 and 4. One can also derive an analogous equation for $f_0\overline{v}^*$:

$$\left[\frac{\partial^2}{\partial y^2}+\frac{1}{\rho_0}\frac{\partial}{\partial z}\left(\rho_0\varepsilon_0\frac{\partial}{\partial z}\right)\right]f_0\overline{v}^*=-\frac{1}{\rho_0}\frac{\partial}{\partial z}\left[\rho_0\varepsilon_0\frac{\partial}{\partial z}\left(\frac{1}{\rho_0}\nabla\cdot\mathbf{F}+\overline{X}\right)\right]$$
$$-\frac{f_0}{\rho_0}\frac{\partial}{\partial z}\left(\frac{\rho_0}{\mathrm{d}\theta_0/\mathrm{d}z}\frac{\partial\overline{\dot{\theta}}}{\partial y}\right). \qquad 26.$$

Comparing the RHS of Equations 25 and 26, one sees that the second-order horizontal derivative of the E-P flux divergence drives the zonal acceleration, whereas the vertical derivative invokes

the residual circulation. Therefore, if the vertical-to-horizontal aspect ratio (h/L) of the E-P flux divergence exceeds f_0/N_0, the wave forcing tends to accelerate the zonal-mean zonal wind rather than be balanced by the Coriolis torque of the residual circulation (Pfeffer 1987, Nakamura & Solomon 2010).

Primitive equations: set of equations that governs the motion of a compressible, hydrostatic atmosphere on a rotating sphere without the quasigeostrophic approximation

Isentropic coordinate: use of potential temperature as the vertical coordinate under hydrostatic balance and stable stratification, wherein diabatic heating becomes "vertical" velocity

Generalized Lagrangian mean (GLM) formalism: formalism in which the mean is defined over a moving material tube; it affords an exact finite-amplitude nonacceleration theorem following the Lagrangian-mean motion of the tube

2.7. Some Generalizations and Limitations

The foregoing formalism was well developed by the early 1980s but has a few limitations. First, the formalism is based on the quasigeostrophic approximation on the Cartesian coordinate and ignores full spherical geometry and nonquasigeostrophic effects such as horizontal variation of static stability. Second, it only depicts the zonally averaged budget of wave activity and zonal-mean zonal wind and remains silent about the longitudinal variation of eddy-mean flow interaction. Finally, the generalized E-P theorem (Equation 16) and the nonacceleration theorem are valid only for small-amplitude eddy.

On the first point, the TEM set and the generalized E-P theorem have been extended to the primitive equations on a rotating sphere through the use of the isentropic coordinate, which simplifies the formalism for the upper troposphere and the lower stratosphere (Andrews 1983, Tung 1986, Held & Schneider 1999). On the other hand, the isentropic coordinate complicates the treatment of the lower boundary where the isentropes intersect the ground. Iwasaki (1989) and Chen (2013) address this by using mass above a given isentropic level as the vertical coordinate.

The formalism has also been extended to describe wave propagation in three dimensions (Hoskins et al. 1983; Plumb 1985, 1986; Takaya & Nakamura 2001; Kinoshita & Sato 2013). The 3D extension of the generalized E-P theorem allows one to track the longitudinal movement of wave train and to infer more precise locations of wave sources from the wave activity fluxes. To remove phase dependence from wave activity and its fluxes, Takaya & Nakamura (2001) combine the two expressions of pseudomomentum (Equation 12) locally. Yet most of these extensions still assume that eddies are of small amplitude and the mean state changes only slowly and mildly.

The small-amplitude requirement of the wave activity equation severely limits its utility for the real atmosphere, where eddy amplitudes are large and the mean state undergoes substantial fluctuations. For example, $\partial\overline{q}/\partial y$ often changes sign once wave amplitude becomes large and hence A_L diverges (Equation 12), and the wave activity budget (Equation 16) is dominated by the $\mathcal{O}(\alpha^3)$ term. This hampers an accurate assessment of the roles of wave transience (wave activity tendency) and wave dissipation in the formation of the E-P flux divergence. Attempts at extending the generalized E-P theorem to finite amplitude were active through the 1970s and 1980s in the fluid mechanics literature. They culminated in the generalized Lagrangian mean (GLM) formalism of Andrews & McIntyre (1978a,c) (see also Grimshaw 1984, Salmon 1988, Bühler 2014), in which wavy displacements of a material tube from its center-of-mass latitude/height are used to define eddy. Unfortunately, the GLM set is difficult to use with gridded meteorological data because the center of mass of a wavy material tube becomes quickly intractable (McIntyre 1980). An Eulerian formalism utilizing impulse-Casimir conservation had some success (Killworth & McIntyre 1985, McIntyre & Shepherd 1987, Haynes 1988), but it also contains a cubic amplitude term that leads to the same issue as the small-amplitude formalism when applied to meteorological data.

Thus, up to this point one still lacks a theoretical framework for finite-amplitude eddy-mean flow interaction applicable to gridded meteorological data for evaluating the angular momentum cycle of eddy and the mean flow. The next section provides an overview of the recent advances to overcome these obstacles. I begin by laying out a diagnostic framework suitable for finite-amplitude eddies on a rotating sphere and demonstrate its applications to data. I limit the scope to the extratropical circulation and assume that it is governed by balanced yet fully nonlinear dynamics under the influence of forcing and dissipation.

3. FINITE-AMPLITUDE WAVE ACTIVITY

Difficulty associated with the Reynolds decomposition like Equation 1 becomes apparent when the eddy amplitude α is large. To the extent that wave activity is defined as an Eulerian field variable and to the extent that it is $\mathcal{O}(\alpha^2)$ at small amplitude, its eddy advective flux is $\mathcal{O}(\alpha^3)$. Unless its divergence vanishes, the budget of wave activity will be quickly dominated by this nonlinear flux as the eddy amplitude grows, obscuring the role of wave transience and wave dissipation.

More fundamentally, when the eddy amplitude is large, the observed zonal-mean state is likely already modified by the eddy effects, so eddy in Equation 1 is not defined relative to a truly eddy-free state. (This is not the case for stationary homogeneous turbulence, in which the eddy fluxes do not alter the mean state.) If a flow were stirred from a condition devoid of eddies, the initial condition could serve as a reference eddy-free state, but for the observed (already highly wavy) atmosphere, such initial condition is not known.

Relabeling symmetry: the fact that for inviscid fluids the principle of stationary action yields the same dynamical equations for all Lagrangian labeling coordinates that preserve density

3.1. Quasi-Conservative Eddy-Free Reference State

Taking a cue from the relabeling symmetry of Hamiltonian fluid mechanics (Virasoro 1981, Griffa 1984, Salmon 1988), Nakamura & Zhu (2010) use the level sets (contours) of PV as a quasi-Lagrangian meridional coordinate to define a hypothetical eddy-free reference state. To describe this process in ways amenable to gridded meteorological data, I adopt the spherical coordinate (longitude λ and latitude ϕ) instead of the Cartesian coordinate (x, y) and rewrite quasigeostrophic PV (Equation 4) as

$$q(\lambda,\phi,z,t) = f + \frac{1}{a\cos\phi}\frac{\partial v}{\partial\lambda} - \frac{1}{a\cos\phi}\frac{\partial(u\cos\phi)}{\partial\phi} + \frac{f}{\rho_0}\frac{\partial}{\partial z}\left(\frac{\rho_0(\theta-\tilde{\theta})}{\partial\tilde{\theta}/\partial z}\right), \qquad 27.$$

where $f = 2\Omega\sin\phi$ is the Coriolis parameter ($\Omega = 7.29\times10^{-5}$ s^{-1} is the rotation rate of the Earth) and $\tilde{\theta}(z,t)$ is hemispheric-mean potential temperature (time dependence is weak). The coordinate transformation obeys $\mathrm{d}x = (a\cos\phi)\mathrm{d}\lambda, \mathrm{d}y = a\mathrm{d}\phi$, where $a = 6{,}378$ km is the planet's radius. ϕ is -0.5π at the South Pole, 0.5π at the North Pole, and 0 at the Equator. Strictly speaking, quasigeostrophic approximation in the spherical coordinate is not dynamically self-consistent. Making f a full function of latitude causes the geostrophic wind to be (slightly) divergent, yet I still treat it as nondivergent. This inconsistency is minor compared to the benefit of finite-amplitude formalism applicable to meteorological data while maintaining the theoretical simplicity of quasigeostrophic dynamics.

Because of the predominance of f in Equation 27, PV is a strong function of latitude, generally increasing from a negative value at the South Pole to a positive value at the North Pole, although it may be wavy in the presence of eddies (**Figure 3*a***). Since PV is materially conserved in the absence of forcing and dissipation, it serves as a quasi-material coordinate for latitude. It is possible to associate the value of PV, Q, with the area $S(Q, t)$ that resides north of that contour,

$$S(Q,z,t) = \iint_{D(Q)} a^2\cos\phi\ \mathrm{d}\lambda\mathrm{d}\phi, \qquad D(Q): q(\lambda,\phi,z,t) \geq Q. \qquad 28.$$

Equation 28 defines one-to-one mapping from the value of PV to area S: $S = 0$ corresponds to the maximum value of Q, and $S = 4\pi a^2$ corresponds to the minimum value. To the extent that winds that advect PV are divergence free and area preserving, $S(Q, z, t)$ is independent of time unless PV has nonadvective sources and sinks. Any time dependence of $S(Q, z, t)$ is a sign that nonconservative processes are altering PV.

One can construct a hypothetical, quasi-conservative, eddy-free reference state by zonalizing the wavy PV contour into a latitude circle without changing the enclosed area. This would be the initial state if the present (wavy) condition evolved conservatively from a zonally symmetric state.

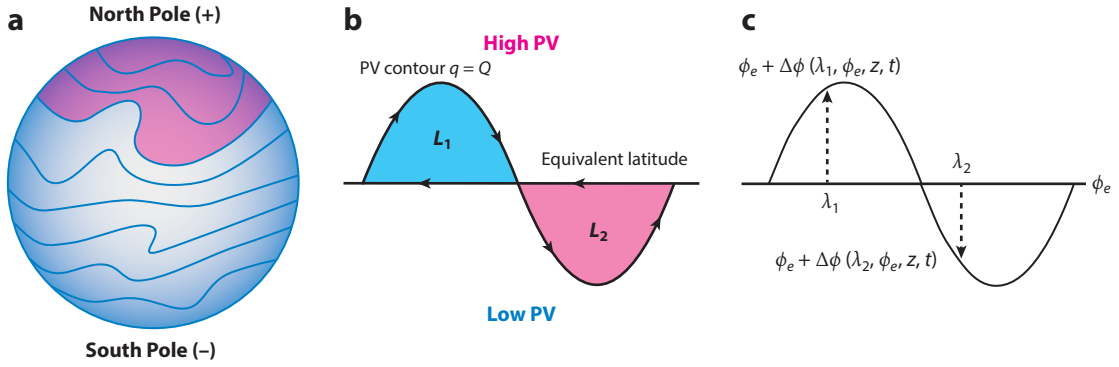

Figure 3

(*a*) Schematic diagram of potential vorticity (PV; denoted by q) distribution on the sphere. (*b*) Lobes enclosed by a wavy PV contour with a value Q ($q = Q$) and the line of latitude that encloses the same area as the PV contour (equivalent latitude, ϕ_e). In lobe L_1, $q \leq Q$ so a negative (clockwise) circulation is induced around it, whereas $q \geq Q$ in L_2 so a positive (counterclockwise) circulation is induced. Areas of L_1 and L_2 are the same by construction. (*c*) Meridional displacement of PV contour from ϕ_e as a function of longitude λ.

Since the reference state is zonally symmetric, it is a function of latitude, height, and time only, and its latitude is related to the area $S(Q, z, t)$ through

$$S(Q, z, t) = 2\pi a^2 (1 - \sin \phi_e). \qquad 29.$$

$\phi_e(Q, z, t)$ is known as equivalent latitude (Butchart & Remsberg 1986, Allen & Nakamura 2003). Q is a monotonic function of ϕ_e for given z and t. Equations 28 and 29 allow Q to be written as a function of ϕ_e, z, and t:

$$Q \equiv Q_{\mathrm{REF}}(\phi_e, z, t). \qquad 30.$$

Note that the mapping of PV onto equivalent latitude is instantaneous and does not depend on the geometry of the PV contours. Contours can be overturned or cut off (in which case all islands are counted as part of a contiguous area). With gridded PV data, the evaluation of the surface integral in Equation 28 is approximated by conditional box counting for the chosen values of Q, and $Q(\phi_e)$ is numerically inverted from $\phi_e(Q)$. Since the area-PV relation does not change under conservative dynamics, the reference-state PV Q_{REF} changes only in response to nonconservative processes. Even though Q_{REF} is zonally symmetric, it shares the same area-PV relationship with the actual (wavy) state, and in that sense it is strongly constrained to the actual climate state.

The reference-state zonal wind u_{REF} and potential temperature θ_{REF} may be inverted hemispherically from Q_{REF} (Pfeffer 1987, Nakamura & Solomon 2010, Nakamura et al. 2020). For the details of this inversion, see the supporting information of Neal et al. (2022) and Section 1 of the **Supplemental Material**. Since u_{REF} is inverted from Q_{REF} and since the latter is invariant under conservative dynamics, any changes in u_{REF} reflect nonadiabatic changes to Q_{REF}. For example, seasonal cycle driven by radiative process and eddy-induced mixing events all affect Q_{REF} and hence u_{REF}. Since u_{REF} is an eddy-free state reachable from the actual (wavy) state through conservative dynamics, the difference between $\overline{u}$ and u_{REF} may be interpreted as the adiabatic effects of eddy on the zonal-mean zonal wind.

Supplemental Material >

Figure 4*a*,*b* shows the Northern Hemisphere monthly mean $\overline{u}$ and u_{REF} for January 2021. While $\overline{u}$ shows a robust subtropical jet (~45 m s^{-1}) in the upper troposphere, u_{REF} in the same region is about 10 m s^{-1} weaker. Therefore, eddies and eddy-induced residual circulation enhance the zonal-mean subtropical jet. However, the greatest difference is in the polar stratosphere, where u_{REF} reaches nearly ~60 m s^{-1} at 30 km but $\overline{u}$ remains weakly negative (easterly). This

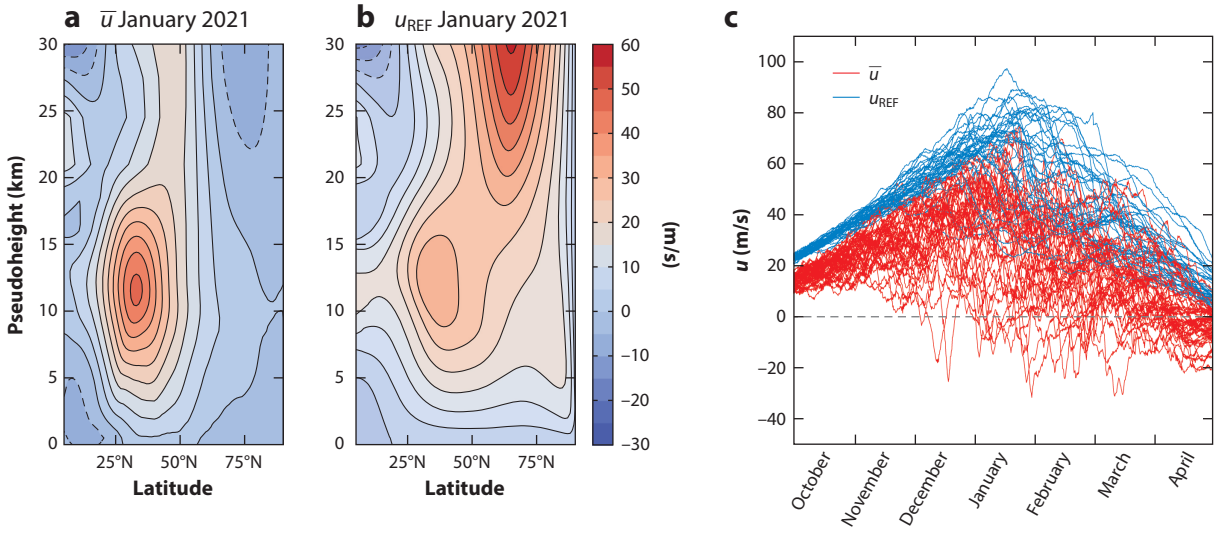

Figure 4

(*a*) Northern Hemisphere monthly mean, zonal-mean zonal wind $\overline{u}$ for January 2021. (*b*) Same as panel *a* but for the reference-state zonal wind u_{REF}. (*c*) Time series of $\overline{u}$ (*red*) and u_{REF} (*blue*) at 60°N 10 hPa (~30 km) for October–April 1979–2020. Data from European Centre for Medium-Range Weather Forecasts Reanalysis v5.

stark difference is a result of the polar vortex being highly distorted and displaced from the pole by a large-amplitude Rossby wave. An example of such event in 2009 is shown in a later figure. **Figure 4*c*** plots time series of u_{REF} and $\overline{u}$ at 60°N 10 hPa ($z \sim 30$ km) during October to April for 42 years. $\overline{u}$ is generally lower than u_{REF} and shows much greater year-to-year variability, including some winters in which $\overline{u}$ is consistently negative. In comparison, u_{REF} shows much less interannual variability, particularly up to December. Thus, u_{REF} captures a canonical seasonal cycle of the polar vortex driven by radiative cooling of the polar region, whereas $\overline{u}$ is much more volatile because of frequent and chaotic large wave events (Nakamura & Solomon 2010). In late winter u_{REF} also becomes somewhat volatile because the mixing process driven by large wave events alters Q_{REF} significantly. (See Equation 53.)

3.2. Eddy-Mean Flow Interaction in Barotropic Flow on a Rotating Sphere

In this subsection, the concept of finite-amplitude Rossby wave activity is introduced using barotropic flow on a rotating sphere as a prototype. The objective is to extend the generalized E-P theorem to finite-amplitude eddies and to describe eddy-mean flow interaction (including dissipative effects) in a way amenable to gridded meteorological data. Generalization to stratified quasigeostrophic flow is straightforward, which is discussed in the next subsection. The governing equation is analogous to Equation 2, but PV (Equation 27) simplifies to absolute vorticity:

$$\frac{Dq}{Dt} = \left(\frac{\partial}{\partial t} + \frac{u}{a\cos\phi}\frac{\partial}{\partial\lambda} + \frac{v}{a}\frac{\partial}{\partial\phi}\right) q = \dot{q}, \tag{31.}$$

$$q(\lambda, \phi, t) = f + \nabla^2\psi, \tag{32.}$$

$$(u, v) = \left(a\cos\phi\ \dot{\lambda},\ a\dot{\phi}\right) = \left(-\frac{1}{a}\frac{\partial\psi}{\partial\phi},\ \frac{1}{a\cos\phi}\frac{\partial\psi}{\partial\lambda}\right). \tag{33.}$$

It is assumed that $\dot{q}$ in Equation 31 represents turbulent diffusion of vorticity.

Polar vortex: strong eastward wind blowing around the polar regions during winter months, normally referring to the seasonal vortex in the stratosphere; athough the term is used more colloquially to describe the upper tropospheric jet stream as well, they are different entities

Figure 3*a* still characterizes the overall spatial distribution of q. Instead of using Equation 1, I define eddy with the meridional displacement of PV from the eddy-free reference state (**Figure 3*b***). Consider a wavy contour of q with the value Q and the corresponding circle of equivalent latitude $\phi = \phi_e(Q)$. The construction of ϕ_e is such that the two curves enclose the equal area on the sphere (Equation 29). Now suppose that the observed (wavy) PV evolved conservatively from the eddy-free reference state; i.e., the PV contour ($q = Q$), was at $\phi = \phi_e$ before the displacement. Then the eddy amplitude may be defined as the amount of PV exchanged across $\phi = \phi_e$ during the displacement, that is, the difference between the surface integral of q over the lobe L_2 displaced to the south of ϕ_e (**Figure 3*b***) and that over the lobe L_1 displaced to the north:

$$\Delta C(\phi_e, t) \equiv \iint_{L_2} qa^2 \cos\phi \mathrm{d}\lambda \mathrm{d}\phi - \iint_{L_1} qa^2 \cos\phi \mathrm{d}\lambda \mathrm{d}\phi, \tag{34.}$$

$$L_1 : q(\lambda, \phi, t) \le Q \text{ and } \phi \ge \phi_e, \qquad L_2 : q(\lambda, \phi, t) \ge Q \text{ and } \phi \le \phi_e. \tag{35.}$$

Since $q \ge Q$ everywhere in L_2 and $q \le Q$ everywhere in L_1, it follows that $\Delta C \ge 0$ and ΔC vanishes only when PV is zonally symmetric (i.e., when the areas of L_1 and L_2 are both zero). Therefore, ΔC is suitable as a metric for eddy amplitude. Note that the definition of ΔC is independent of the shape of the PV contours and therefore applies to eddies with arbitrary amplitudes (waves or turbulent eddies). Equation 34 may be written in an alternative form,

$$\Delta C(\phi_e, t) = C_1(Q(\phi_e, t)) - C_2(\phi_e, t), \tag{36.}$$

$$C_1(Q(\phi_e, t)) \equiv \iint_{D_1} qa^2 \cos\phi \mathrm{d}\lambda \mathrm{d}\phi, \qquad D_1 : q(\lambda, \phi, t) \ge Q(\phi_e, t), \tag{37.}$$

$$C_2(\phi_e, t) \equiv \iint_{D_2} qa^2 \cos\phi \mathrm{d}\lambda \mathrm{d}\phi, \qquad D_2 : \phi \ge \phi_e. \tag{38.}$$

Finite-amplitude Rossby wave activity is then defined as

$$A(\phi_e, t)\cos\phi_e \equiv \frac{\Delta C}{2\pi a} = \frac{1}{2\pi a}(C_1 - C_2) \ge 0. \tag{39.}$$

The two integrals in Equations 37 and 38 are readily calculable from gridded data using conditional box counting. It can be shown that $A\cos\phi_e$ approaches $A_L\cos\phi$ (Equation 12) in the limit of small-amplitude eddy (Nakamura & Zhu 2010, Solomon & Nakamura 2012), while $A\cos\phi_e$ does not involve $\partial\overline{q}/\partial\phi$ and remains finite even when the latter changes sign.

Figure 5 depicts evolution of $q(\lambda, \phi, t)$, $A_L(\phi, t)\cos\phi$, and $A(\phi_e, t)\cos\phi_e$ during a barotropic decay experiment on a rotating sphere. The model setup follows Held & Phillipps (1987) and solves Equation 31 with $\dot{q}$ being small numerical viscosity. Eddy is initially concentrated in the midlatitudes and superposed on a stable zonal jet. As the eddy radiates meridionally as Rossby waves, they encounter critical lines on the flanks of the jet and break, and the contours of PV (absolute vorticity) turn over (**Figure 5*a–d***). This produces a local reversal of $\partial\overline{q}/\partial\phi$ and consequently a singular behavior in $A_L\cos\phi$ (Equation 12), limiting its utility as a diagnostic (**Figure 5*e***). In contrast, $A\cos\phi_e$ avoids this problem and correctly identifies the meridional separation of wave activity and its accumulation in the critical layers (**Figure 5*f***). Although the overall patterns of $A_L\cos\phi$ and $A\cos\phi_e$ are similar, clearly the latter offers a more meaningful diagnostic at finite amplitude. On the other hand, the accuracy of $A\cos\phi_e$ may be compromised at small amplitude, as it is computed as a difference of two large integrals (Equation 39).

Because C_1 and C_2 are surface integrals of absolute vorticity (Equations 37 and 38), by the Stokes theorem, they are equivalent to Kelvin's circulation around the wavy PV contour and

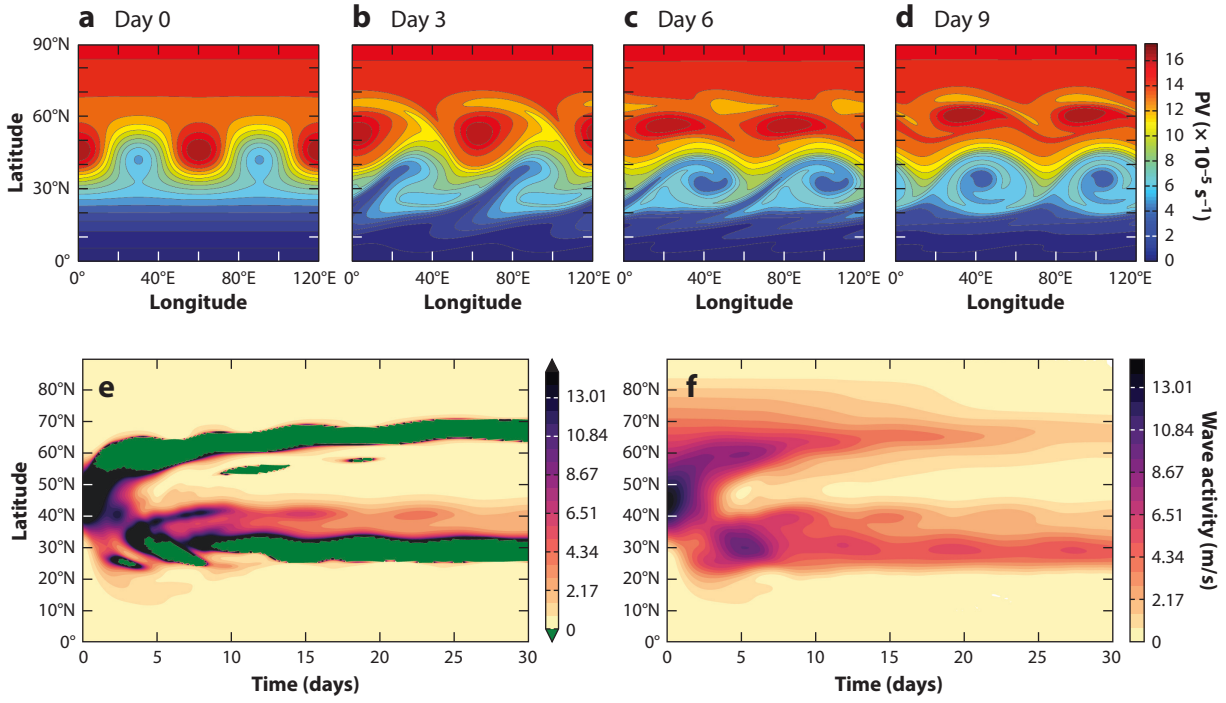

Figure 5

(*a–d*) Evolution of potential vorticity (PV) (absolute vorticity) during barotropic decay experiment on a rotating sphere for days 0, 3, 6, and 9. The model setup follows equations 2 and 3 of Held & Phillipps (1987) with an initial eddy vorticity amplitude $\zeta_0 = 8 \times 10^{-5}$ s^{-1}. Due to zonal symmetry (wavenumber 6), only one-third of the domain is shown. (*e*) Latitude-time cross section for linear wave activity $A_L \cos\phi$ during the experiment. The green regions are where the zonal-mean PV gradient is negative and/or A_L is exceedingly large. (*f*) Same as panel *e* but for finite-amplitude wave activity $A \cos\phi_e$. Figure adapted with permission from Huang (2017); copyright Clare S.Y. Huang.

around the line of equivalent latitude, respectively. Under conservative dynamics ($\dot{q} = 0$) PV is materially conserved so the PV contour is a material line. Therefore, C_1 becomes a constant of motion (Kelvin's circulation theorem):

$$\frac{\partial C_1(\phi_e, t)}{\partial t} = 0. \qquad 40.$$

Meanwhile, from Equation 38,

$$\frac{\partial C_2(\phi_e, t)}{\partial t} = 2\pi a \cos\phi_e \overline{v'q'}, \qquad 41.$$

where $\overline{v'q'}$ denotes the zonal-mean meridional advective flux of vorticity across the latitude line $\phi = \phi_e$. Then from Equations 14 and 39–41,

$$\frac{\partial A \cos\phi_e}{\partial t} = -\cos\phi_e \overline{v'q'} = -\frac{1}{\rho_0} \nabla \cdot \mathbf{F}, \qquad 42.$$

where $\mathbf{F} = \rho_0 \cos\phi(0, -\overline{u'v'}, 0)$ is the E-P flux in spherical coordinate (ρ_0 may be considered constant in barotrophic flow) and $-\rho_0^{-1} \nabla \cdot \mathbf{F} = (a \cos\phi_e)^{-1} \partial(\overline{u'v'} \cos^2\phi)/\partial\phi$. Equation 42 is a finite-amplitude extension to Equation 16 for barotropic flow in the conservative limit ($\mathcal{D} = 0$). Most notably, unlike Equation 16, there is no cubic term in eddy amplitude: This term has been absorbed in the new definition of wave activity.

Since C_2 is absolute circulation around the latitude circle at $\phi = \phi_e$ (Equation 38),

$$C_2(\phi_e, t) = 2\pi a \cos\phi_e (\Omega a \cos\phi_e + \overline{u}(\phi_e, t)), \tag{43.}$$

Effective diffusivity: diffusion coefficient amplified by the effects of fluid stirring; calculated from the gradient structure of a tracer field governed by advection-diffusion; stirring (strain) increases the local tracer gradient and stretches the tracer isosurface, both of which act to enhance effective diffusivity

where Ω is the rotation rate of the sphere. Substitution in Equation 41 then yields

$$\frac{\partial \overline{u}\cos\phi_e}{\partial t} = \cos\phi_e \overline{v'q'} = \frac{1}{\rho_0}\nabla \cdot \mathbf{F}. \tag{44.}$$

Equation 44 is analogous to Equation 20, but there is no residual circulation because the zonal-mean meridional velocity identically vanishes in barotropic flow. Thus, in the absence of friction, angular momentum of the zonal-mean flow is solely driven by the eddy PV flux (the E-P flux divergence). Then from Equations 42 and 44

$$\frac{\partial \overline{u}}{\partial t} = -\frac{\partial A}{\partial t}. \tag{45.}$$

Therefore, the zonal-mean zonal wind will not accelerate without a change in wave activity (wave transience). This is a fully finite-amplitude statement of nonacceleration theorem. Equation 45 also suggests that $\overline{u}(\phi_e, t) + A(\phi_e, t)$ is a constant under conservative dynamics. In fact, from Equations 39 and 43,

$$\overline{u} + A = \frac{1}{2\pi a \cos\phi_e} C_1 - \Omega a \cos\phi_e \equiv u_{\mathrm{REF}}(\phi_e), \tag{46.}$$

where C_1 is a constant of motion [Kelvin's circulation (Equation 40)]. If a wave packet arrives from elsewhere and changes an eddy-free state (u_{REF}, 0) to a wavy state ($\overline{u}, A$) ($A > 0$) conservatively, then $\overline{u} < u_{\mathrm{REF}}$ from Equation 46; that is, zonal-mean zonal wind must be decelerated. That the wave packet decelerates the zonal flow means that the Rossby wave carries negative angular pseudomomentum density: $-Aa\cos\phi_e < 0$. [It also means that a negative (westward) zonal torque must be added to the fluid to excite Rossby waves.] Once the wave packet exits the region, the eddy-free state will be restored—that is, eddy-mean flow interaction under a conservative dynamics is reversible. By integrating Equations 42 and 44 globally and using the fact that $\nabla \cdot \mathbf{F}$ integrates to zero,

$$\frac{\mathrm{d}}{\mathrm{d}t}\int \overline{u} a^2 \cos^2\phi_e \mathrm{d}\phi_e = -\frac{\mathrm{d}}{\mathrm{d}t}\int A a^2 \cos^2\phi_e \mathrm{d}\phi_e = 0. \tag{47.}$$

This is a statement of the volume conservation of angular momentum and angular pseudomomentum. The latter may be used for deriving a sufficient condition for modal stability of the flow at finite amplitude (Shepherd 1988, Nakamura & Zhu 2010).

When there is turbulent mixing (diffusion) $\dot{q} = -\nabla \cdot \mathbf{F}_{\mathrm{d}}$, where $\mathbf{F}_{\mathrm{d}}$ is diffusive flux of vorticity, C_1 becomes time dependent and (with Equation 37, and the divergence theorem)

$$\frac{\partial C_1(Q,t)}{\partial t} = \iint_{D_1} \dot{q} a^2 \cos\phi \mathrm{d}\lambda \mathrm{d}\phi = -\oint_Q \mathbf{F}_{\mathrm{d}} \cdot \mathbf{n}\, \mathrm{d}l, \tag{48.}$$

where $\mathbf{n} \equiv -\nabla q/|\nabla q|$. The RHS quantifies the diffusive loss of vorticity out of the domain D_1 (Equation 37). Using ϕ_e as a coordinate, Equation 48 may be written as (Nakamura & Zhu 2010)

$$\frac{\partial C_1(\phi_e, t)}{\partial t} = -2\pi K_{\mathrm{eff}} \cos\phi_e \frac{\partial Q_{\mathrm{REF}}}{\partial \phi_e}, \tag{49.}$$

where $K_{\mathrm{eff}}(\phi_e, t)$ is effective diffusivity of PV across its own contour and $Q_{\mathrm{REF}}(\phi_e, t)$ denotes the zonalized reference PV field (Equation 30). See Nakamura (1996, 2008) and Nakamura & Zhu (2010) for the definition of K_{eff} and derivation of Equation 49 from Equation 48.

Meanwhile, assuming that the zonal-mean diffusive flux of vorticity is small compared to the advective flux in a high–Reynolds number flow, Equations 41 and 44 remain intact, provided that there is no additional frictional torque. Then from Equations 14, 39, 41, and 49,

$$\frac{\partial A \cos\phi_e}{\partial t} = -\frac{1}{\rho_0}\nabla\cdot\mathbf{F} - K_{\text{eff}}\cos\phi_e\frac{1}{a}\frac{\partial Q_{\text{REF}}}{\partial\phi_e}. \quad 50.$$

The last term is nonpositive because $K_{\text{eff}} \geq 0$ and $\partial Q_{\text{REF}}/\partial\phi_e > 0$. It represents wave dissipation due to mixing (enstrophy dissipation). From Equations 44 and 50 one obtains, instead of Equation 45,

$$\frac{\partial\overline{u}}{\partial t} = -\frac{\partial A}{\partial t} - \frac{K_{\text{eff}}}{a}\frac{\partial Q_{\text{REF}}}{\partial\phi_e}. \quad 51.$$

Therefore, in the presence of mixing ($K_{\text{eff}} > 0$), both wave transience and wave dissipation affect eddy-mean flow interaction (McIntyre & Norton 1990). Integrating Equation 51 over a time period $t \in [t_0, t_1]$,

$$\Delta\overline{u} = -\Delta A - \int_{t_0}^{t_1}\frac{K_{\text{eff}}}{a}\frac{\partial Q_{\text{REF}}}{\partial\phi_e}\mathrm{d}t. \quad 52.$$

Thus, even if there is no secular variation in wave activity ($\Delta A = 0$), the zonal-mean zonal wind will be decelerated irreversibly ($\Delta\overline{u} < 0$) because wave dissipation causes negative pseudomomentum to be left behind. The reference-state wind $u_{\text{REF}} = \overline{u} + A$ also becomes time dependent, since Kelvin's circulation in Equation 46 is no longer a constant of motion:

$$\frac{\partial u_{\text{REF}}}{\partial t} = -\frac{K_{\text{eff}}}{a}\frac{\partial Q_{\text{REF}}}{\partial\phi_e}. \quad 53.$$

However, the difference between $\overline{u}$ and u_{REF} is solely governed by wave transience,

$$\frac{\partial}{\partial t}(\overline{u} - u_{\text{REF}}) = -\frac{\partial A}{\partial t}. \quad 54.$$

This suggests that the partitioning of the mean flow into u_{REF} and $\overline{u} - u_{\text{REF}}$ will help compare the relative effects of wave dissipation and wave transience.

3.3. Eddy-Mean Flow Interaction in Stratified Quasigeostrophic Flow

It is straightforward to extend the foregoing formalism to stratified quasigeostrophic flow. Wave activity is evaluated at each altitude in the same way as the barotropic case using quasigeostrophic PV instead of absolute vorticity. Thus, in the calculation of C_1 and C_2 in Equations 37–39, q is defined by Equation 27. Equation 50 remains the same except that $\mathbf{F}$ is now redefined as Equation 15 times $\cos\phi$, and there is an additional term associated with the diabatic source of PV. For conciseness, all nonconservative sources and sinks of wave activity will be lumped into $\dot{A}\cos\phi_e$:

$$\frac{\partial A\cos\phi_e}{\partial t} = -\frac{1}{\rho_0}\nabla\cdot\mathbf{F} + \dot{A}\cos\phi_e. \quad 55.$$

Equation 55 is a finite-amplitude extension to the generalized E-P theorem (Equation 16).

Meanwhile, in the spherical coordinate, Equation 20 is modified to

$$\frac{\partial}{\partial t}\overline{u}\cos\phi_e = f\overline{v}^*\cos\phi_e + \frac{1}{\rho_0}\nabla\cdot\mathbf{F} + \overline{X}\cos\phi_e. \quad 56.$$

In the conservative limit ($\dot{A} = \overline{X} = 0$), Equations 56 and 55 give

$$\frac{\partial\overline{u}}{\partial t} - f\overline{v}^* = -\frac{\partial A}{\partial t}. \quad 57.$$

Unlike Equation 45, wave transience is related not only to the deceleration of the zonal-mean zonal wind but also to the Coriolis torque of the residual circulation. To get better sense of Equation 57, note that it differs from

$$\left(\frac{\partial}{\partial t}+\frac{\overline{v}^*}{a}\frac{\partial}{\partial \phi_e}\right)\left(\overline{u}\cos\phi_e+\Omega a\cos^2\phi_e\right)=-\left(\frac{\partial}{\partial t}+\frac{\overline{v}^*}{a}\frac{\partial}{\partial \phi_e}\right)\left(A\cos\phi_e\right) \qquad 58.$$

only by an order of Rossby number (which is small under quasigeostrophic scaling); that is, $\mathcal{O}(\overline{u}/\Omega a\cos\phi_e)\approx\mathcal{O}\left(A/\Omega a\cos\phi_e\right)\ll 1$. Thus, to within the accuracy of quasigeostrophic approximation, Equation 58 states that the absolute angular momentum of the zonal-mean state does not change following the residual circulation $\overline{v}^*$ unless wave activity changes on the same path. This is a nonlocal statement of nonacceleration theorem. With Equation 46 it is clear that Equation 58 also states material conservation of Kelvin's circulation C_1 following $\overline{v}^*$ (to be more precise, C_1 here should be called pseudocirculation since it is an area integral of quasigeostrophic PV, not absolute vorticity, conserved on isobaric surface, not isentropic surface). Baroclinic extension to the nonacceleration theorem (Equations 53 and 54) is expressed in Equations 5 and 6 of the **Supplemental Material**.

Supplemental Material >

Figure 6 shows the behavior of PV and streamfunction (**Figure 6*a–d***) and the relationships between $A\cos\phi_e$ and $(\overline{u}-u_{\mathrm{REF}})\cos\phi_e$ (**Figure 6*e***) and between $A\cos\phi_e$ and $u_{\mathrm{REF}}\cos\phi_e$ (**Figure 6*f***) during the stratospheric sudden warming event in 2009 (Harada et al. 2010). During this event, the circumpolar vortex is disrupted, split, and dissipated by a large-amplitude planetary Rossby wave propagating from the troposphere over the course of a few weeks (**Figure 6*a–d***). The circumpolar winds reversed from strong westerlies to weak easterlies. Leading up to the peak of the event, $(\overline{u}-u_{\mathrm{REF}})\cos\phi_e$ decreases linearly with an increasing $A\cos\phi_e$. After the vortex splits, $A\cos\phi_e$ decreases while $(\overline{u}-u_{\mathrm{REF}})\cos\phi_e$ recovers, tracing nearly the same path as the lead (**Figure 6*e***). The behavior of $u_{\mathrm{REF}}\cos\phi_e$, on the other hand, is distinctly irreversible. It stays nearly steady until the vortex splits; after that it declines steadily as a result of enhanced mixing, and it does not recover even after $A\cos\phi_e$ decays (**Figure 6*f***). Thus, the partition of the flow into $\overline{u}-u_{\mathrm{REF}}$ and u_{REF} indeed quantifies the separate signals of wave transience and dissipation during this highly nonlinear event.

Although in **Figures 4*c*** and **6*e***, $\overline{u}-u_{\mathrm{REF}}<0$ for $A\cos\phi_e>0$, that is not always the case for baroclinic flow because of the residual circulation. For example, in **Figure 4*a*,*b*** $\overline{u}-u_{\mathrm{REF}}>0$ around the subtropical jet in the upper troposphere. As stated in Section 2.6, wave transience has less ability to decelerate the flow when the aspect ratio of eddy forcing is small (shallow) (Pfeffer 1987, Nakamura & Solomon 2010).

4. LOCAL WAVE ACTIVITY

Finite-amplitude wave activity developed in the previous section extends the generalized E-P theorem and the associated nonacceleration theorem to eddies with arbitrary amplitudes. Yet it is an overall measure of waviness of PV for a given latitude and height; it does not describe longitudinal variation of waviness. Meteorological events are often geographically localized, and hence it is desirable to generalize wave activity as a function of longitude to characterize eddy-mean flow interaction on regional scales. To this end, Huang & Nakamura (2016) define the meridional displacement of PV at each longitude as

$$A^*(\lambda,\phi_e,z,t)\cos\phi_e\equiv -a\int_0^{\Delta\phi(\lambda,\phi_e,z,t)} q_e(\lambda,\phi_e,\phi',z,t)\cos(\phi_e+\phi')\mathrm{d}\phi', \qquad 59.$$

$$q_e(\lambda,\phi_e,\phi',z,t)=q(\lambda,\phi_e+\phi',z,t)-Q_{\mathrm{REF}}(\phi_e,z,t), \qquad 60.$$

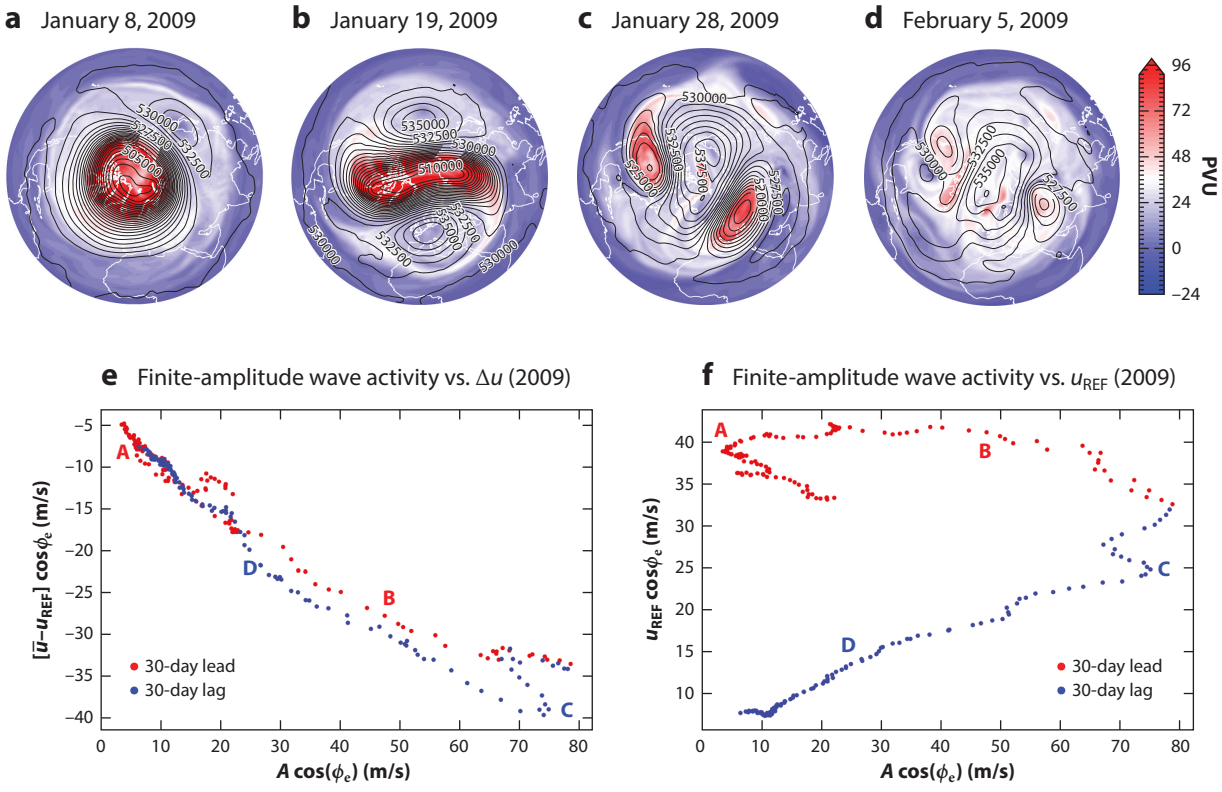

Figure 6

(*a–d*) Polar projection of potential vorticity (PV) (*color*, 1 PVU = 10^{-6} m^2 s^{-1} K kg^{-1}) and Montgomery streamfunction (*contours* every 1,250 m^2 s^{-2}) on 850-K isentropic surface (pseudoheight $z \sim 32$ km) during the 2009 stratospheric sudden warming. (*a*) January 8. (*b*) January 19. (*c*) January 28. (*d*) February 5. (*e*) Finite-amplitude wave activity $A\cos\phi_e$ (abscissa) versus the departure of the zonal-mean angular momentum from the reference-state angular momentum $(\bar{u} - u_{\mathrm{REF}})\cos\phi_e$ (ordinate) at equivalent latitude $\phi_e = 60°$N, $z =$ 32 km during the same event (30-day lead plus 30-day lag). Labels A–D correspond to the timing of panels *a–d*. (*f*) Same as panel *e* but $A\cos\phi_e$ versus $u_{\mathrm{REF}}\cos\phi_e$. Figure adapted with permission from Nakamura et al. (2020); copyright American Meteorological Society.

where $\Delta\phi$ denotes the meridional displacement of the wavy PV contour relative to the line of equivalent latitude ϕ_e at longitude λ (**Figure 3*c***). q_e is the difference between PV and its reference-state value at ϕ_e ($Q = Q_{\mathrm{REF}}$), and $A^*\cos\phi_e$ is the line integral (weighted by $\cos\phi$) of q_e from $\phi = \phi_e + \Delta\phi$ to ϕ_e (along the dashed lines in **Figure 3*c***). $\phi' \in [0, \Delta\phi]$ is a displacement coordinate to perform this integral. In the lobe L_1 of **Figure 3*b***, $q \le Q = Q_{\mathrm{REF}}$, thus $q_e \le 0$ whereas $\Delta\phi > 0$; therefore, $A^*\cos\phi_e \ge 0$. In L_2, $q_e \ge 0$ and $\Delta\phi < 0$, so again $A^*\cos\phi_e \ge 0$. Thus, $A^*\cos\phi_e$ is positive regardless of the direction of the displacement. Where the PV contour is overturned, the integral path may intersect the contour multiple times, changing the sign of q_e. In this case the integral is performed over all segments of the path in which q_e takes the correct sign. Defined this way, $A^*\cos\phi_e$ amounts to the longitude-by-longitude contribution to $A\cos\phi_e$ (Equation 39) in the sense that the zonal average of the former recovers the latter (for derivation, see Huang & Nakamura 2016): $\overline{A^*}\cos\phi_e = A(\phi_e, z, t)\cos\phi_e$. Huang & Nakamura (2016) call $A^*\cos\phi_e$ finite-amplitude local wave activity (strictly speaking, local wave activity is local only in longitude but nonlocal in latitude). In the small-amplitude limit, $A^*\cos\phi_e$ approaches $a\cos\phi_e q'^2(2\partial\overline{q}/\partial\phi)^{-1}$ (the limit considered by Plumb 1986).

Figure 1*b* shows a snapshot of local wave activity in the upper troposphere corresponding to **Figure 1*a***. Generally speaking, local wave activity is large where the jet stream is displaced meridionally and small along the axis of the jet. Wave activity tends to form lumps at the troughs and ridges of the jet stream, and they collectively migrate eastward. Note that local wave activity and its budget are defined at each longitude and therefore contain phase structure of the Rossby waves. Thus, local wave activity may be used to detect phase-specific weather events (e.g., an anomalously strong trough or ridge in the westerlies). It is distinct from pseudomomentum density of a wave packet (amplitude envelope), which is defined as a phase-averaged quantity. The phase variation of local wave activity may be removed by moderate spatial and/or temporal smoothing to analyze the behavior of a Rossby wave packet (e.g., Ghinassi et al. 2018).

4.1. Column Budget of Local Wave Activity

Supplemental Material >

The governing equation for local wave activity may be obtained by taking the time derivative of Equation 59, substituting the PV equation, and applying the Leibniz rule repeatedly (Huang & Nakamura 2016) (see also Section 3 of the **Supplemental Material**):

$$\frac{\partial A^* \cos\phi_e}{\partial t} = -\frac{1}{\rho_0}\left(\nabla \cdot \mathbf{F}_{\rm adv} + \nabla \cdot \mathbf{F}_{\rm EP}\right) + \dot{A}^* \cos\phi_e, \tag{61.}$$

$$\mathbf{F}_{\rm adv} \equiv \rho_0 \left[u_{\rm REF} A^* \cos\phi_e - a\int_0^{\Delta\phi} u_e q_e \cos(\phi_e + \phi')\mathrm{d}\phi', 0, 0 \right], \tag{62.}$$

$$\mathbf{F}_{\rm EP} \equiv \rho_0 \cos\phi\ v_e q_e = \rho_0 \cos\phi \left[\frac{1}{2}\left(v_e^2 - u_e^2 - \frac{R}{H}\frac{e^{-\kappa z/H}\theta_e^2}{\partial\tilde{\theta}/\partial z}\right), -u_e v_e, \frac{f v_e \theta_e}{\partial\tilde{\theta}/\partial z}\right], \tag{63.}$$

where the departure from the reference state (u_e, v_e, θ_e) is defined in a similar way to q_e (Equation 60) and $\dot{A}^*$ is nonconservative sources and sinks of A^*. The reference state is inverted from $Q_{\rm REF}$ as described in Section 1 of the **Supplemental Material**. Equation 61 is a 3D extension to Equation 55 (zonal average of Equation 61 recovers Equation 55), and it governs the evolution of local wave activity (opposite of angular pseudomomentum density). $\mathbf{F}_{\rm adv}$ and $\mathbf{F}_{\rm EP}$ denote the advective flux of wave activity and 3D radiation stress, respectively. Notice that the advective flux involves only the longitudinal component, since the meridional advection is absorbed in the tendency of wave activity through displacements of PV. An analogous result for small-amplitude wave activity is derived by Plumb (1986).

In the troposphere, there is a significant difference in the vertical structures of wave activity and the zonal wind (Nakamura & Solomon 2010), and often their covariation becomes evident only after taking the vertical average (Wang & Nakamura 2015). With the density-weighted vertical average denoted by angle brackets, Equation 61 becomes

$$\frac{\partial \langle A^* \rangle \cos\phi_e}{\partial t} = \underbrace{-\frac{1}{a\cos\phi_e}\frac{\partial}{\partial\lambda}\langle F_\lambda\rangle}_{\rm I} \underbrace{+\frac{1}{a\cos\phi_e}\frac{\partial}{\partial\phi}\left(\langle u_e v_e\rangle \cos^2\phi\right)\Big|_{\phi=\phi_e}}_{\rm II}$$
$$\underbrace{+\frac{f}{H}\frac{v_e\theta_e\cos\phi_e}{\partial\tilde{\theta}/\partial z}\Big|_{z=0}}_{\rm III} \underbrace{+\langle\dot{A}^*\rangle\cos\phi_e}_{\rm IV}, \tag{64.}$$

$$\langle F_\lambda\rangle \equiv \langle u_{\rm REF} A^*\rangle \cos\phi_e - a\left\langle \int_0^{\Delta\phi} u_e q_e \cos(\phi_e+\phi')\mathrm{d}\phi' \right\rangle$$
$$+\frac{1}{2}\left\langle v_e^2 - u_e^2 - \frac{R}{H}\frac{e^{-\kappa z/H}\theta_e^2}{\partial\tilde{\theta}/\partial z}\right\rangle \cos\phi_e. \tag{65.}$$

Terms I and II in Equation 64 denote the zonal and meridional convergence of the column-mean wave activity flux, whereas term III denotes the wave activity source at the surface, and term IV is the nonconservative sources/sinks. The left-hand side (LHS) and terms I–III may be evaluated from gridded meteorological data, whereas term IV is commonly computed as the residual of the budget (Huang & Nakamura 2017; Neal et al. 2022; H.-I. Lee, N. Nakamura, submitted manuscript). Because of the density weighting in the vertical average, the column budget mainly samples the troposphere. In the time mean and global mean, the LHS and terms I and II vanish so the primary balance is between terms III (positive) and IV (negative): As depicted in **Figure 2**, wave activity enters the atmosphere at the surface and is dissipated in the interior.

In Section 4 of the **Supplemental Material**, seasonal climatology of column-mean local wave activity and its budget is analyzed for the Northern Hemisphere winter. The analysis generalizes **Figure 2** and reveals regional sources and sinks of Rossby wave activity, as well as the horizontal transmission of wave activity between them.

Atmospheric blocking: abnormally large and stationary meandering of the jet stream that disrupts the normal eastward progression of weather systems in the midlatitudes, often causing regional extreme weather

Supplemental Material >

4.2. Regional Eddy-Mean Flow Interaction

Compared to Equations 45 and 51, the local relationship between wave activity and zonal wind involves more terms (even after column average), and their action-reaction relation is not immediately obvious (Huang & Nakamura 2016). Nevertheless, there is a robust negative correlation between the observed column-mean local wave activity and zonal wind (Wang & Nakamura 2015, Nakamura & Huang 2018). **Figure 7*a*** shows the covariance of $\langle A^* \rangle \cos\phi_e$ and $\langle u \rangle \cos\phi_e$ for the Northern Hemisphere winter. The covariance is everywhere negative but is particularly strong over the eastern Pacific and eastern Atlantic in the exit regions of the jet stream. The peak covariance occurs slightly south to the peak wave activity values (**Supplemental Figure 1*a***), and these locations define the hotspots for eddy-flow interaction. Scatter plots constructed for the locations of peak covariance clearly show that the regional condition of the atmosphere swings between the state with a strong westerly wind and small wave activity and the state with a weak (or reversed) westerly wind and large wave activity (**Figure 7*b*,*c***).

5. EDDY-MEAN FLOW INTERACTION AND ATMOSPHERIC BLOCKING

Figure 8 shows composites of winter tropospheric circulation for the anomalous large wave events identified in **Figure 7*b*,*c***. A stationary wave with zonal wavenumber 2 is evident in geopotential height, and the locations identified in **Figure 7*a*** are both in the vicinity of the stationary ridges. The composites reveal anomalous meandering of the jet stream around these locations, with markedly enhanced wave activity values slightly to the north (**Figure 8*a*,*b***). These are characteristics of atmospheric blocking, a main cause for weather extremes in the extratropics (Woollings et al. 2018, Lupo 2021, Kautz et al. 2022). Blocking events are notoriously difficult to predict, and despite the improvement in forecast skills, they still cause occasional forecast busts (Rodwell et al. 2013). Forecasts tend to exhibit strong sensitivity to the initial condition before a blocking event (Matsueda 2011). So what drives such anomalous behavior of the jet stream, and can it be understood in terms of local wave activity dynamics?

Analysis of meteorological data reveals the following two points (Nakamura & Huang 2018):

- Wave activity budget (Equation 64) in the hotspots of eddy-flow interaction is dominated by the LHS and term I on short timescales (days).
- The second term on the RHS of Equation 65 is predominantly negative and quickly overwhelms the positive first term as wave activity grows.

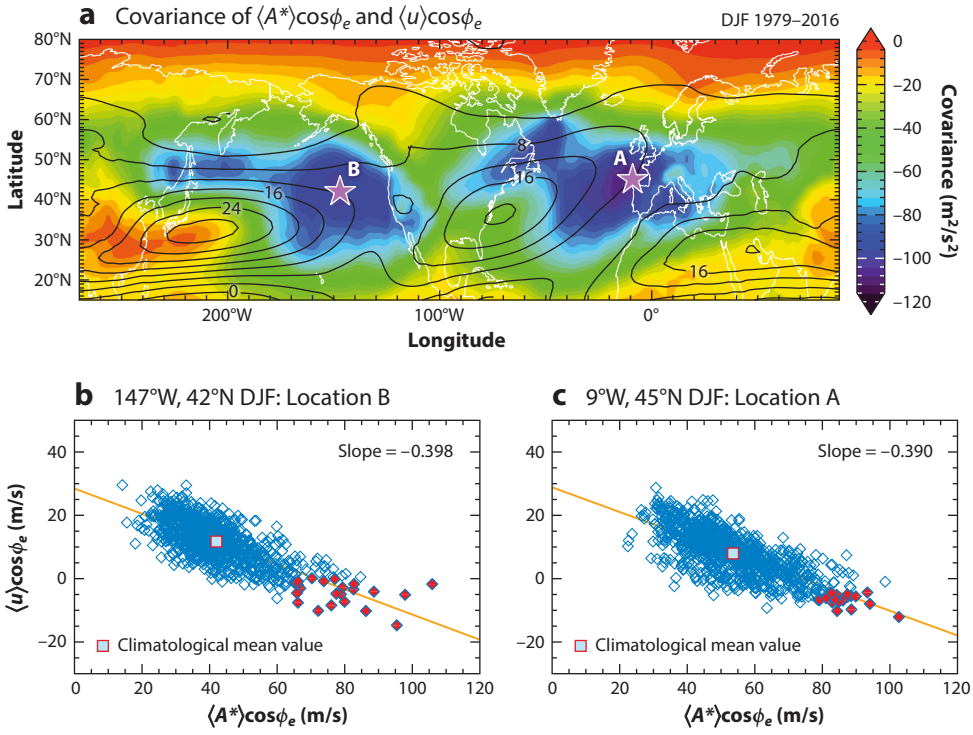

Figure 7

(*a*) Covariance of column-mean local wave activity $\langle A^* \rangle \cos \phi_e$ and zonal wind $\langle u \rangle \cos \phi_e$ for the boreal winter [December, January, and February (DJF); *color*]. Contours indicate climatological values of $\langle u \rangle \cos \phi_e$ in m/s. The locations of peak covariance are labeled A (9°W 45°N) and B (147°W 42°N). (*b*) Scatter diagrams of 4-day averaged $\langle A^* \rangle \cos \phi_e$ and $\langle u \rangle \cos \phi_e$ at location B. The red diamonds are the instances when $\langle A^* \rangle \cos \phi_e$ and $\langle u \rangle \cos \phi_e$ are simultaneously in the top and bottom 5 percentile, respectively, of all 853 sampled values. The orange line is the least square fit with the value of slope indicated. (*c*) Same as panel *b* but for location A. Figure adapted from Nakamura & Huang (2018).

Based on these observations, the following idealization to Equations 64 and 65 may be adopted:

$$\frac{\partial A^*}{\partial t} = -\frac{\partial F_x}{\partial x} + S - \frac{A^*}{\tau}, \qquad 66.$$

$$F_x = U_0 A^* - \alpha A^{*2} + c_g A^*, \qquad 67.$$

where S, τ, U_0, α, c_g are all positive constants. The cosine factor and angle bracket have been dropped. To go from Equation 64 to Equation 66, only the zonal flux convergence is explicitly modeled and the remaining (unimportant) terms are parameterized as external forcing and linear damping. From Equation 65 to Equation 67, the first and second terms are approximated as $(U_0 - \alpha A^*)A^*$, while the last term is approximated as group velocity c_g times wave activity. The key element is that the advecting wind $U_0 - \alpha A^*$ decreases with increasing wave activity (**Figure 7*b*,*c***), which represents the regional eddy-flow interaction. Because of this, the flux F_x becomes a nonlinear function of wave activity. (If small viscosity is added, Equation 66 may be linearized using the Cole-Hopf transformation, but the resultant form of the solution does not elucidate physics, so it is not employed here.) Furthermore, wave activity A^* may be partitioned

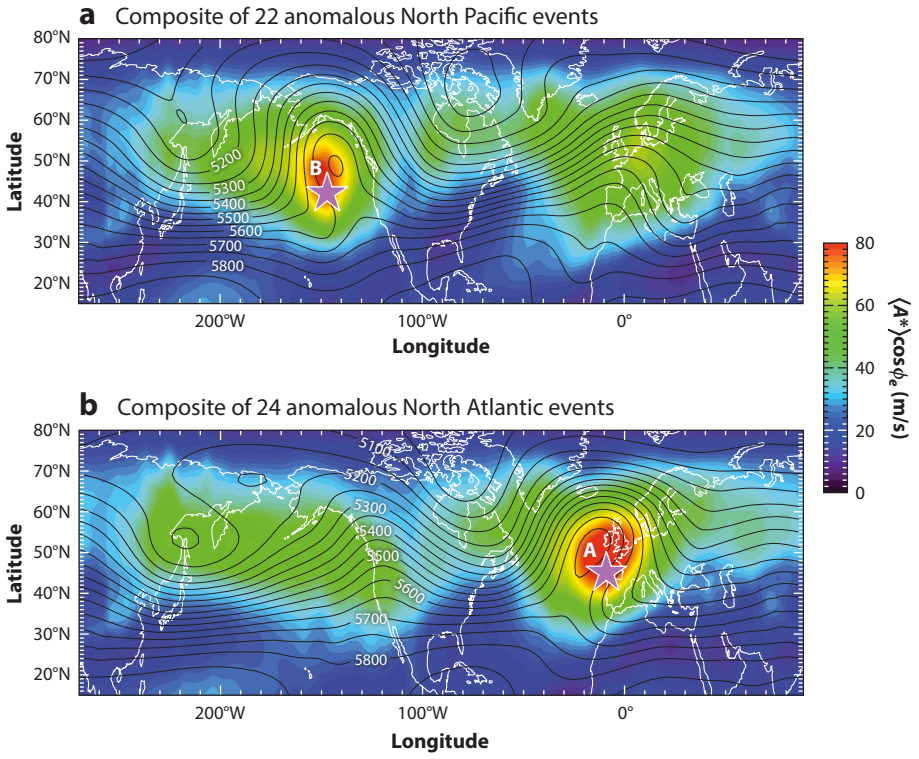

Figure 8

(*a*) Northern Hemisphere column-mean local wave activity $\langle A^* \rangle \cos\phi_e$ (*color*) and 500 hPa geopotential height (*contours* in meters) for a composite of 22 anomalous Pacific events marked in red in **Figure 7*b***. (*b*) Same as panel *a* but a composite of 24 anomalous Atlantic events in **Figure 7*c***. The stars (A, B) correspond to the locations marked in **Figure 7*a***. Figure adapted from Nakamura & Huang (2018).

Supplemental Material >

into the baseline (steady) component $A_0(x)$ and the transient component $\hat{A}(x,t)$ (**Supplemental Figure 1*b*,*c***) $A^*(x,t) = A_0(x) + \hat{A}(x,t)$. Substituting in Equation 66, one obtains

$$\frac{\partial \hat{A}}{\partial t} = -\frac{\partial}{\partial x}\left[\left(C(x) - \alpha\hat{A}\right)\hat{A}\right] + \hat{S} - \frac{\hat{A}}{\tau}, \qquad 68.$$

$$C(x) = U_0 + c_g - 2\alpha A_0(x). \qquad 69.$$

The effective advecting wind $C(x)$ for the transient wave activity is modulated by the stationary wave $A_0(x)$, and $C(x)$ is weaker where $A_0(x)$ is large. The flux of transient wave activity $(C(x) - \alpha\hat{A})\hat{A}$ increases with $\hat{A}$ when $\hat{A}$ is small, but due to nonlinearity it peaks at $C^2/4\alpha$ when $\hat{A}$ reaches the critical value of $C/2\alpha \equiv \hat{A}_{\text{crit}}$, and beyond that the flux decreases with increasing $\hat{A}$. If $\hat{A}$ exceeds $\hat{A}_{\text{crit}}$ somewhere, the flux begins to decrease, and if the incident flux from upstream does not change, it creates flux convergence and hence further increases $\hat{A}$. Because of this positive feedback, as long as the incident flux is sustained, $\hat{A}$ surges to C/α, at which point the flux vanishes and the wave stalls.

This stalling mechanism is mathematically equivalent to traffic congestion on a highway if one reinterprets $\hat{A}$ as traffic density (Lighthill & Whitham 1955, Richards 1956, Nakamura & Huang

2018). As traffic density increases, the drivers' braking frequency increases and the traffic speed decreases. As a result, beyond a critical value of traffic density, the traffic flux decreases and a jam ensues quickly. $C(x)$ corresponds to the speed limit or the number of open lanes on a highway, and where $C(x)$ is small, $\hat{A}_{\rm crit} = C/2\alpha$ is also small, making the location prone to congestion. Viewed this way, it is natural to liken atmospheric blocking to a traffic jam on the highway—the weather highway of the jet stream. That the preferred regions of blocking coincide with the exit regions of the jet stream is also consistent with the traffic theory. **Figure 9** shows simple 1D and 2D numerical experiments in which waves traveling along a PV front encounter a diffluent flow and exceed the critical value of wave activity (Nakamura & Huang 2017). When this happens the wave envelope develops a sudden jump (shock), and it slowly migrates upstream, as the stagnant region expands by absorbing the incident flux.

The idea that wave transience occurs when the flux of wave activity reaches the carrying capacity of the flow may be applicable to other large wave events such as wave breaking and stratospheric sudden warming (see related discussions by Fyfe & Held 1990, Wang & Fyfe 2000, Nakamura et al. 2020). The argument does not require the preexistence of critical lines (Dickinson 1968, 1970), yet the absorption of wave activity into a stagnant region (**Figure 9**) is akin to the critical layer behavior of the meridionally propagating Rossby waves (Killworth & McIntyre 1985).

6. CONCLUSIONS

The purpose of this rather technical review was to demonstrate how the principles of fluid dynamics may be applied to the Earth's extratropical atmosphere to advance our understanding of large-scale circulation and assist the interpretation of meteorological data. The focus of the article was how finite-amplitude Rossby waves and geostrophic eddies interact with the mean flow and redistribute angular momentum (and heat) within the atmosphere.

The most recent advances in this area entail two aspects. The first concerns an extension of wave activity conservation [the generalized E-P theorem (Equation 16)] to finite amplitude in a way amenable to gridded meteorological data (Section 3). Rather than seeking a most general theory, making a judicious choice of quasi-Lagrangian coordinate helps achieve this goal. Specifically, eddy has been redefined in terms of displacement of PV with respect to a quasi-conservative reference state. The reference state is constructed by zonalizing the wavy PV field through an area preserving map (Section 3.1). It is invariant under adiabatic, frictionless dynamics and in reality only slowly evolves in response to seasonal radiative forcing and mixing processes. The new formulation simplifies the conservation equation for wave activity and makes it easy to evaluate the relative importance of wave transience and wave dissipation/forcing in the modification of the mean flow. Meanwhile, the TEM set that governs the zonal-mean state is not altered at all by the finite-amplitude wave activity formalism.

The second aspect concerns the localization of wave activity to identify regional sources and sinks of Rossby waves and their transmission between those regions (Section 4; Section 4 in the **Supplemental Material**). Local wave activity is introduced as a longitude-by-longitude contribution to finite-amplitude wave activity. Local wave activity budget, when combined with regional eddy-mean flow interaction, elucidates how wave transience and large-amplitude events such as atmospheric blocking might emerge (Section 5). In the governing equation of local wave activity, a higher-order term in eddy amplitude appears only in the zonal advective flux of wave activity, and this term plays a key role in causing stagnation of the jet stream through regional eddy-mean flow interaction. An idealized model based on the observed budget of local wave activity suggests that blocking arises when the flow's carrying capacity for wave activity is reached. If this is how large wave events (and associated extreme weather) occur in the extratropics, one may be able to project

Supplemental Material >

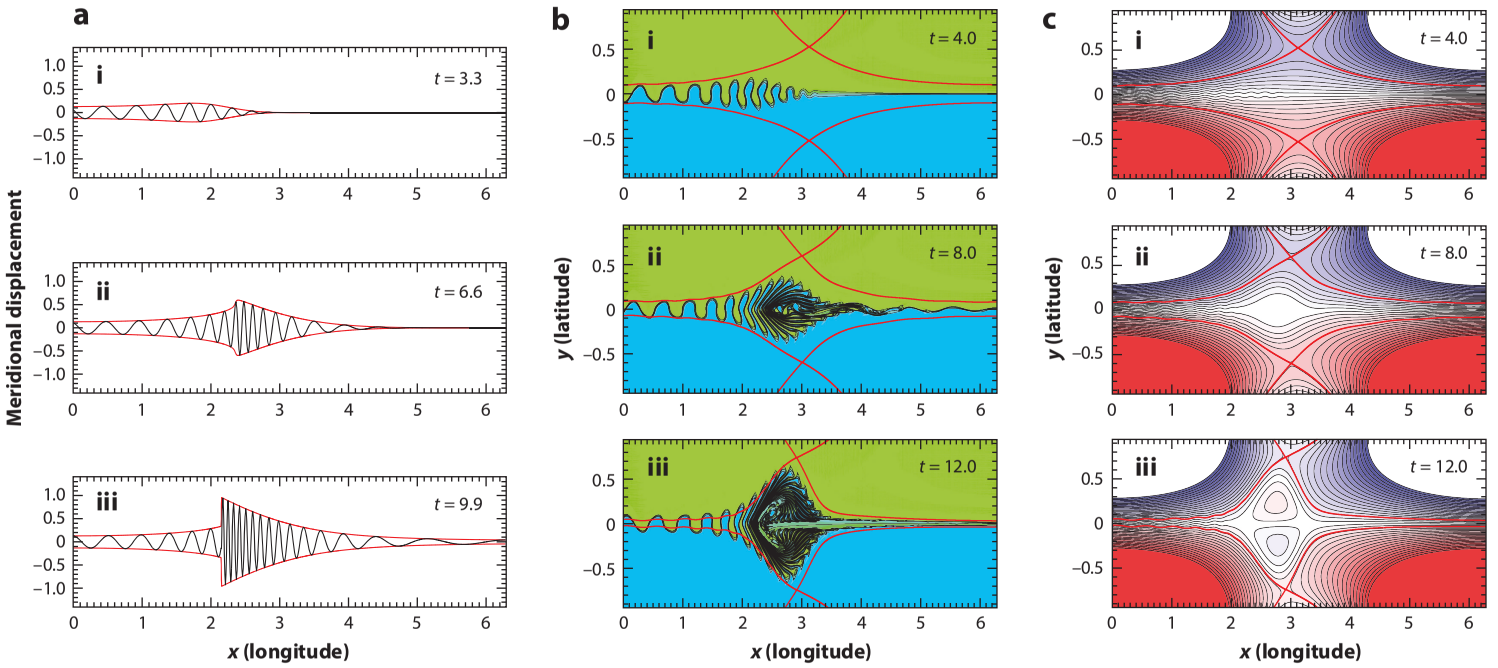

Figure 9

Idealized numerical experiments of atmospheric blocking. The incident wave from the left encounters a slow background wind in the middle of the channel. (*a*) 1D: evolution of the longitudinal structure of a wave traveling along a potential vorticity (PV) front. From *i* to *iii*: $t = 3.3, 6.6, 9.9$ (t is nondimensional time). Horizontal axis (x) is nondimensional longitude. Critical amplitude is exceeded at $x \approx 2.4$, $t = 6.6$. (*b*) 2D: structure of PV associated with a wave packet traveling along the PV front. x- and y-axes denote nondimensional longitude and latitude, respectively. From *i* to *iii*: $t = 4, 8, 12$. Critical value is exceeded at $x \approx 2.4$, $t = 6.6$. (*c*) Streamfunction corresponding to panel *b*. Figure adapted with permission from Nakamura & Huang (2017); copyright American Meteorological Society.

Supplemental Material >

Quasi-biennial oscillation: alternating appearance of easterly and westerly winds in the equatorial stratosphere with a period of about 28 months

how climate change might affect the frequency and strength of large wave events by studying the sensitivity of carrying capacity. Section 5 of the **Supplemental Material** demonstrates the usage of the 1D traffic flow model for this purpose.

Although I chose to work within the framework of quasigeostrophic dynamics to keep the theoretical interpretation simple, most of the conclusions about finite-amplitude Rossby waves are generalizable to the primitive equations, particularly if one adopts Kelvin's circulation theorem in isentropic coordinate (Nakamura & Solomon 2011, Methven & Berrisford 2015, Ghinassi et al. 2018). It is important to point out that, while the Rossby waves and geostrophic eddies play dominant roles in the extratropics, they are not the only agents of eddy-mean flow interaction in the atmosphere. For example, equatorial waves (particularly gravity waves) drive the well-documented quasi-biennial oscillation in the equatorial stratosphere (Lindzen & Holton 1968, Holton & Lindzen 1972, Plumb 1977, Baldwin et al. 2001). Gravity waves are also important in exerting drag in the zonal wind in the upper atmosphere (Lindzen 1981, Fritts & Alexander 2003). Wave-mean flow interaction involving gravity waves is more complex than that for Rossby waves because gravity waves are bidirectional. Pseudomomentum (hence wave activity) of gravity waves can take either sign depending on their propagation speed (Equation 12). Still, some of the concepts discussed in this article (e.g., carrying capacity of wave activity flux in relation to wave breaking) likely transcend wave types and are applicable to gravity waves as well.

DISCLOSURE STATEMENT

The author is not aware of any biases that might be perceived as affecting the objectivity of this review.

ACKNOWLEDGMENTS

The author thanks the organizers and participants of the Workshop on Transport and Mixing of Tracers in Geophysics and Astrophysics at the Aspen Center for Physics in June 2021, where some of the ideas presented in this article were consolidated. Discussions with Phil Morrison, Paul Kushner, James Cho, Albion Lawrence, Jean-Luc Thiffeault, and Jeff Weiss were particularly helpful. This work has been supported by National Science Foundation grants 1909522 and 2154523. Python codes to evaluate wave activity and the reference state from reanalysis data may be found at **https://github.com/csyhuang/hn2016_falwa** courtesy of Clare Huang.

LITERATURE CITED

Allen DR, Nakamura N. 2003. Tracer equivalent latitude: a diagnostic tool for isentropic transport studies. *J. Atmos. Sci.* 60:287–304

Andrews DG. 1983. A finite-amplitude Eliassen-Palm theorem in isentropic coordinates. *J. Atmos. Sci.* 40:1877–83

Andrews DG, Holton JR, Leovy CB. 1987. *Middle Atmosphere Dynamics*. San Diego/London: Academic

Andrews DG, McIntyre ME. 1976. Planetary waves in horizontal and vertical shear: the generalized Eliassen-Palm relation and the mean zonal acceleration. *J. Atmos. Sci.* 33:2031–48

Andrews DG, McIntyre ME. 1978a. An exact theory of nonlinear waves on a Lagrangian-mean flow. *J. Fluid Mech.* 89:609–46

Andrews DG, McIntyre ME. 1978b. Generalized Eliassen-Palm and Charney-Drazin theorems for waves on axisymmetric mean flows in compressible atmospheres. *J. Atmos. Sci.* 35:175–85

Andrews DG, McIntyre ME. 1978c. On wave-action and its relatives. *J. Fluid Mech.* 89:647–64

Baldwin MP, Gray LJ, Dunkerton TJ, Hamilton K, Haynes PH, et al. 2001. The quasi-biennial oscillation. *Rev. Geophys.* 39:179–229

Boyd JP. 1976. The noninteraction of waves with the zonally averaged flow on a spherical Earth and the interrelationships on eddy fluxes of energy, heat and momentum. *J. Atmos. Sci.* 33:2285–91
Bretherton FP, Garrett CJR. 1968. Wavetrains in inhomogeneous moving media. *Proc. R. Soc. A* 302:529–54
Bühler O. 2014. *Waves and Mean Flows*. Cambridge, UK: Cambridge Univ. Press. 2nd ed.
Butchart N, Remsberg EE. 1986. The area of the stratospheric polar vortex as a diagnostic for tracer transport on an isentropic surface. *J. Atmos. Sci.* 43:1319–39
Charney JG. 1947. The dynamics of long waves in a baroclinic westerly current. *J. Atmos. Sci.* 4:136–62
Charney JG. 1948. On the scales of atmospheric motions. *Geofys. Publ.* 18:3–17
Charney JG. 1971. Geostrophic turbulence. *J. Atmos. Sci.* 28:1087–95
Charney JG, Drazin PG. 1961. Propagation of planetary-scale disturbances from the lower into the upper atmosphere. *J. Geophys. Res.* 66(1):83–109
Chen G. 2013. The mean meridional circulation of the atmosphere using the mass above isentropes as the vertical coordinate. *J. Atmos. Sci.* 70:2197–223
Dickinson RE. 1968. Planetary Rossby waves propagating vertically through weak westerly wind wave guides. *J. Atmos. Sci.* 25:984–1002
Dickinson RE. 1970. Development of a Rossby wave critical level. *J. Atmos. Sci.* 27:627–33
Eady ET. 1949. Long waves and cyclone waves. *Tellus* 1:33–52
Edmon HJ, Hoskins BJ, McIntyre ME. 1980. Eliassen-Palm cross sections for the troposphere. *J. Atmos. Sci.* 37:2600–16
Eliassen A. 1951. Slow thermally or frictionally controlled meridional circulations in a circular vortex. *Astrophys. Norv.* 5:19–60
Eliassen A, Palm E. 1961. On the transfer of energy in stationary mountain waves. *Geofys. Publ.* 22:1–23
Fritts DC, Alexander MJ. 2003. Gravity wave dynamics and effects in the middle atmosphere. *Rev. Geophys.* 41:1003
Fyfe J, Held IM. 1990. The two-fifths and one-fifth rules for Rossby wave breaking in the WKB limit. *J. Atmos. Sci.* 47:697–706
Ghinassi P, Fragkoulidis G, Wirth V. 2018. Local finite-amplitude wave activity as a diagnostic for Rossby wave packets. *Mon. Wea. Rev.* 146:4099–114
Griffa A. 1984. Canonical transformations and variational principles for fluid dynamics. *Physica A* 127:265–81
Grimshaw R. 1984. Wave action and wave-mean flow interaction, with application to stratified shear flows. *Annu. Rev. Fluid Mech.* 16:11–44
Harada Y, Goto A, Hasegawa H, Fujikawa N, Naoe H, Hirooka T. 2010. A major stratospheric sudden warming event in January 2009. *J. Atmos. Sci.* 67:2052–69
Hartmann DL. 2015. *Global Physical Climatology*. Amsterdam: Elsevier. 2nd ed.
Haurwitz B. 1940. The motion of atmospheric disturbances. *J. Mar. Res.* 3:35–50
Haynes PH. 1988. Forced, dissipative generalizations of finite-amplitude wave-activity conservation relations for zonal and nonzonal basic flows. *J. Atmos. Sci.* 45:2352–62
Held IM. 1983. Stationary and quasi-stationary eddies in the extratropical troposphere: theory. In *Large-Scale Dynamical Processes in the Atmosphere*, ed. B Hoskins, R Pearce, pp. 127–68. New York: Academic
Held IM, Hoskins BJ. 1985. Large-scale eddies and the general circulation of the troposphere. *Adv. Geophys.* 28(Part A):3–31
Held IM, Phillipps PJ. 1987. Linear and nonlinear barotropic decay on the sphere. *J. Atmos. Sci.* 44:200–7
Held IM, Scheider T. 1999. The surface branch of the zonally averaged mass transport circulation in the troposphere. *J. Atmos. Sci.* 56:1688–97
Hersbach H, Bell B, Berrisford P, Hirahara S, Horányi A, et al. 2020. The ERA5 global reanalysis. *Q. J. R. Meteorol. Soc.* 146:1999–2049
Holton JR, Lindzen RS. 1972. An updated theory for the quasi-biennial cycle of the tropical stratosphere. *J. Atmos. Sci.* 29:1076–80
Hoskins BJ, James IN, White GH. 1983. The shape, propagation and mean-flow interaction of large-scale weather systems. *J. Atmos. Sci.* 40:1595–612
Hoskins BJ, Karoly DJ. 1981. The steady linear response of a spherical atmosphere to thermal and orographic forcing. *J. Atmos. Sci.* 38:1179–96

Huang CSY. 2017. *Finite-amplitude local wave activity as a diagnostic of anomalous weather events*. PhD Thesis, Univ. Chicago

Huang CSY, Nakamura N. 2016. Local finite-amplitude wave activity as a diagnostic of anomalous weather events. *J. Atmos. Sci.* 73:211–29

Huang CSY, Nakamura N. 2017. Local wave activity budgets of the wintertime Northern Hemisphere: implication for the Pacific and Atlantic storm tracks. *Geophys. Res. Lett.* 44:5673–82

Iwasaki T. 1989. A diagnostic formulation for wave-mean flow interactions and Lagrangian-mean circulation with a hybrid vertical coordinate of pressure and isentrope. *J. Meteorol. Soc. Jpn.* 67:293–312

Jeffreys H. 1926. On the dynamics of geostrophic winds. *Q. J. R. Meteorol. Soc.* 51:85–101

Kautz LA, Martius O, Pfahl S, Pinto JG, Ramos AM, et al. 2022. Atmospheric blocking and weather extremes over the Euro-Atlantic sector—a review. *Weather Clim. Dynam.* 3:305–36

Killworth PD, McIntyre ME. 1985. Do Rossby-wave critical layers absorb, reflect, or over-reflect? *J. Fluid Mech.* 161:449–92

Kinoshita T, Sato K. 2013. A formulation of unified three-dimensional wave activity flux of inertia–gravity waves and Rossby waves. *J. Atmos. Sci.* 70:1603–15

Kuo H. 1956. Forced and free meridional circulations in the atmosphere. *J. Meteorol.* 13:561–68

Lighthill MJ, Whitham GB. 1955. On kinematic waves II. A theory of traffic flow on long crowded roads. *Proc. R. Soc. A* 229:317–45

Lindzen RS. 1981. Turbulence and stress owing to gravity wave and tidal breakdown. *J. Geophys. Res.* 86(C10):9707–14

Lindzen RS, Holton JR. 1968. A theory of the quasi-biennial oscillation. *J. Atmos. Sci.* 25:1095–107

Longuet-Higgins MS. 1965. Planetary waves on a rotating sphere. II. *Proc. R. Soc. A* 284:40–68

Lorenz EN. 1955. Available potential energy and the maintenance of the general circulation. *Tellus* 7:157–67

Lupo AR. 2021. Atmospheric blocking events: a review. *Ann. N. Y. Acad. Sci.* 1504:5–24

Matsueda M. 2011. Predictability of Euro-Russian blocking in summer of 2010. *Geophys. Res. Lett.* 38:L06801

Matsuno T. 1971. A dynamical model of the stratospheric sudden warming. *J. Atmos. Sci.* 28:1479–94

McIntyre ME. 1980. An introduction to the generalized Lagrangian-mean description of wave, mean-flow interaction. *Pure Appl. Geophys.* 118:152–76

McIntyre ME, Norton WA. 1990. Dissipative wave-mean interactions and the transport of vorticity or potential vorticity. *J. Fluid Mech.* 212:403–35

McIntyre ME, Shepherd TG. 1987. An exact local conservation theorem for finite-amplitude disturbances to non-parallel shear flows, with remarks on Hamiltonian structure and on Arnol'd's stability theorems. *J. Fluid Mech.* 181:527–65

Methven J, Berrisford P. 2015. The slowly evolving background state of the atmosphere. *Q. J. R. Meteorol. Soc.* 141:2237–58

Nakamura N. 1996. Two-dimensional mixing, edge formation, and permeability diagnosed in an area coordinate. *J. Atmos. Sci.* 53:1524–37

Nakamura N. 2008. Quantifying inhomogeneous, instantaneous, irreversible transport using passive tracer field as a coordinate. In *Transport and Mixing in Geophysical Flows*, ed. JB Weiss, A Provenzale, pp. 137–64. Berlin: Springer-Verlag

Nakamura N, Faulk J, Lubis SW. 2020. Why are stratospheric sudden warmings sudden (and intermittent)? *J. Atmos. Sci.* 77:943–64

Nakamura N, Huang CSY. 2017. Local wave activity and the onset of blocking along a potential vorticity front. *J. Atmos. Sci.* 74:2341–62

Nakamura N, Huang CSY. 2018. Atmospheric blocking as a traffic jam in the jet stream. *Science* 361:42–47

Nakamura N, Solomon A. 2010. Finite-amplitude wave activity and mean flow adjustments in the atmospheric general circulation. Part I: quasigeostrophic theory and analysis. *J. Atmos. Sci.* 67:3967–83

Nakamura N, Solomon A. 2011. Finite-amplitude wave activity and mean flow adjustments in the atmospheric general circulation. Part II: analysis in the isentropic coordinate. *J. Atmos. Sci.* 68:2783–99

Nakamura N, Zhu D. 2010. Finite-amplitude wave activity and diffusive flux of potential vorticity in eddy–mean flow interaction. *J. Atmos. Sci.* 67:2701–16

Neal E, Huang CSY, Nakamura N. 2022. The 2021 Pacific Northwest heat wave and associated blocking: meteorology and the role of an upstream cyclone as a diabatic source of wave activity. *Geophys. Res. Lett.* 49:e2021GL097699

Palmén E. 1949. Meridional circulations and the transfer of angular momentum in the atmosphere. *J. Meteorol.* 6:429–30

Pfeffer RL. 1987. Comparison of conventional and transformed Eulerian diagnostics in the troposphere. *Q. J. R. Meteorol. Soc.* 113:237–54

Phillips NA. 1951. A simple three-dimensional model for the study of large-scale extratropical flow patterns. *J. Meteorol.* 8:381–94

Platzman GW. 1968. The Rossby wave. *Q. J. R. Meteorol. Soc.* 94:225–48

Plumb RA. 1977. The interaction of two internal waves with the mean flow: implications for the theory of the quasi-biennial oscillation. *J. Atmos. Sci.* 34:1847–58

Plumb RA. 1985. On the three-dimensional propagation of stationary waves. *J. Atmos. Sci.* 42:217–29

Plumb RA. 1986. Three-dimensional propagation of transient quasi-geostrophic eddies and its relationship with the eddy forcing of the time–mean flow. *J. Atmos. Sci.* 43:1657–78

Rhines PB. 1975. Waves and turbulence on a beta-plane. *J. Fluid. Mech.* 69:417–43

Richards PI. 1956. Shock waves on the highway. *Oper. Res.* 4:42–51

Rodwell MJ, Magnusson L, Bauer P, Bechtold P, Bonavita M, et al. 2013. Characteristics of occasional poor medium-range weather forecasts for Europe. *Bull. Am. Meteorol. Soc.* 94:1393–405

Rossby CG. 1939. Relation between variations in the intensity of the zonal circulation of the atmosphere and the displacements of the semi-permanent centers of action. *J. Mar. Res.* 2:38–55

Rossby CG, Starr V. 1949. Interpretation of the angular momentum principle as applied to the general circulation of the atmosphere. *J. Meteorol.* 6:288

Salmon R. 1980. Baroclinic instability and geostrophic turbulence. *Geophys. Astrophys. Fluid Dyn.* 15:167–211

Salmon R. 1988. Hamiltonian fluid mechanics. *Annu. Rev. Fluid Mech.* 20:225–56

Shepherd TG. 1988. Nonlinear saturation of baroclinic instability. Part I: the two-layer model. *J. Atmos. Sci.* 45:2014–25

Solomon A, Nakamura N. 2012. An exact Lagrangian-mean wave activity for finite-amplitude disturbances to barotropic flow on a sphere. *J. Fluid Mech.* 693:69–92

Starr V. 1949. Meridional circulations and the transfer of angular momentum in the atmosphere—reply. *J. Meteorol.* 6:430

Starr V. 1968. *Physics of Negative Viscosity Phenomena*. New York: McGraw-Hill

Takaya K, Nakamura H. 2001. A formulation of a phase-independent wave-activity flux for stationary and migratory quasigeostrophic eddies on a zonally varying basic flow. *J. Atmos. Sci.* 58:608–27

Tung KK. 1986. Nongeostrophic theory of zonally averaged circulation. Part I: formulation. *J. Atmos. Sci.* 43:2600–18

Vallis GK. 2017. *Atmospheric and Oceanic Fluid Dynamics: Fundamentals and Large-Scale Circulation*. Cambridge, UK: Cambridge Univ. Press. 2nd ed.

Virasoro MA. 1981. Variational principle for two-dimensional incompressible hydrodynamics and quasi-geostrophic flows. *Phys. Rev. Lett.* 47:1181–83

Wallace JM, Battisti DS, Thompson DWJ, Hartmann DL. 2023. *The Atmospheric General Circulation*. Cambridge, UK: Cambridge Univ. Press

Wang L, Nakamura N. 2015. Covariation of finite-amplitude wave activity and the zonal mean flow in the midlatitude troposphere: 1. Theory and application to the Southern Hemisphere summer. *Geophys. Res. Lett.* 42:8192–200

Wang X, Fyfe J. 2000. Onset of edge wave breaking in an idealized model of the polar stratospheric vortex. *J. Atmos. Sci.* 57:956–66

Woollings T, Barriopedro D, Methven J, Son SW, Martius O, et al. 2018. Blocking and its response to climate change. *Curr. Clim. Change Rep.* 4:287–300